15
Elastic recovery

15.1 Introduction

The extent to which a fibre becomes permanently deformed when it is stretched is of great technical importance. It may be just as serious a form of damage as actual breakage of the fibre. The values of stress and strain above which permanent deformation occurs may well be the limiting values in use. In some specialised applications, such as ropes used in rock-climbing, the fibres may safely be taken beyond their yield point once, but their properties will then be so altered that they are unfit for further use.

Elastic recovery, that is, the behaviour on removal of stress, is only a special case of the general phenomenon of hysteresis. In a cyclic change of stress or strain, the results will not fall on a single line. After a few initial cycles, the fibre will become conditioned and the results will tend to fall on a loop, as in Fig. 15.1. This means that energy is used up by internal friction, and consequently the material will heat up and may tend to dry out. This is important where fibres are subject to repeated loading, as in tyres, and the heating will affect their properties. In these uses, fibres showing little hysteresis are desirable.

On a molecular scale, recoverable or elastic deformation is due to a stretching of inter-atomic and intermolecular bonds, as in Fig. 15.2(b), while non-recoverable or plastic deformations result from a breaking of bonds and their re-forming in new positions, Fig. 15.2(c), or to the stabilisation of new chain conformations.

As with other tensile properties, recovery is time dependent. This leads to hysteresis, even if, after time, the recovery is complete. Although creep is defined as elongation

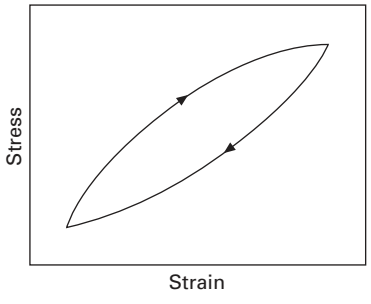

15.1 Hysteresis loop.

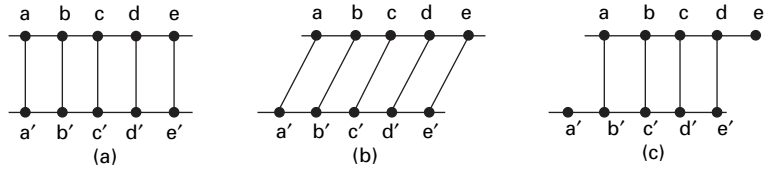

15.2 Schematic illustration of elastic and plastic deformations: (a) initial configuration; (b) elastic deformation with straining of links; (c) plastic deformation with re-forming of links in new positions.

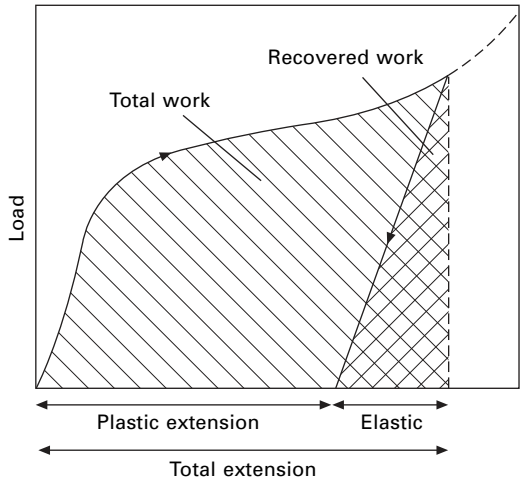

15.3 Elastic and plastic extension.

under constant load, part of the elongation under increasing load can be regarded as slow 'creep', which is followed by slow 'creep recovery'.

15.2 Definitions

Elasticity, a much misused word, has been defined by the American Society for Testing and Materials as 'that property of a body by virtue of which it tends to recover its original size and shape after deformation'. Its opposite is plasticity. It should not be used as synonymous with extensibility.

A deformation may be divided up, as shown in Fig. 15.3, into an elastic part, which is recovered when the stress is removed, and a plastic or permanent part. Quantitatively, it is convenient to use the following definition:

$$\text{elastic recovery} = \frac{\text{elastic extension}}{\text{total extension}}$$

Complete recovery will then have the value 1 (or 100%), incomplete recovery will have a proportionately lower fraction, and no recovery at all will have the value zero.

Instead of studying dimensional recovery, one may study and define work recovery in a similar manner:

$$\text{work recovery} = \frac{\text{work returned during recovery}}{\text{total work done in extension}}$$

It should be noted that (1– work recovery) gives the proportion of the total work that is dissipated as heat.

15.3 Experimental methods

The method used by Meredith [1] in his classic series of comparative tests, is typical of experiments on elastic recovery, though Instron-type testers would now be used. He studied the same fibres as he had used in tests of their tensile properties.

In measurements of recovery, the particular programme of application and removal of stress is important. Meredith used the Cliff constant-rate-of-loading tester and applied the load at a rate of 10 gf/(den min) (0.15 mN/(tex s). When the required load had been reached, it was left on the specimen for 2 min. The load was taken off at the same rate and left off until 1 min after the start of unloading. The procedure was then repeated for higher loads. Preliminary experiments had shown that this timing was the minimum that would give a reasonable approach to equilibrium. Tests were made at stresses of 0.3, 0.5, 1, 2, 2.5, 3, 4 and 5 gf/den (26.7, 44.5, 89, 198, 222.5, 267, 396, 445 mN/tex) (up to break) and at the yield stress. The results were found to be little affected by test-length. A 1.5 cm length was used for short fibres and a 5 cm length for long fibres. The relative humidity was 65% and the temperature 20 °C.

Figure 15.4 gives a typical record obtained in the tests and shows the division into elastic and permanent extensions. From this, the elastic recovery can be calculated. Note the extension and recovery at constant stress due to creep during the dwell periods. In an Instron test at constant rate of extension, there would be a decrease of stress at constant extension due to stress relaxation, as shown in Figure 15.5.

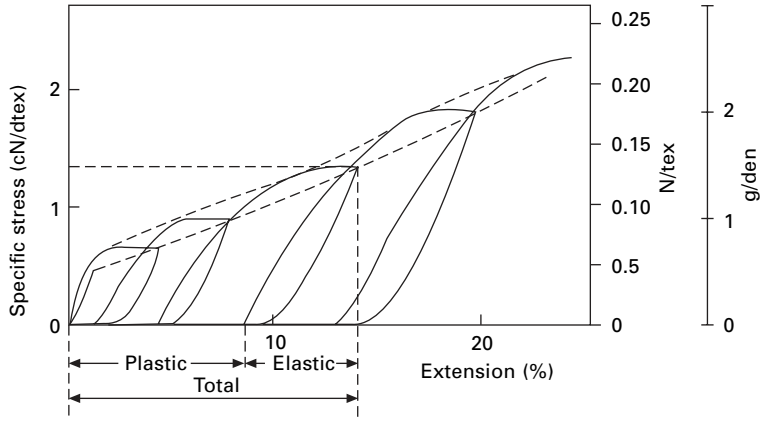

15.4 Stress–strain curves of viscose rayon in loading and unloading. After Meredith [1].

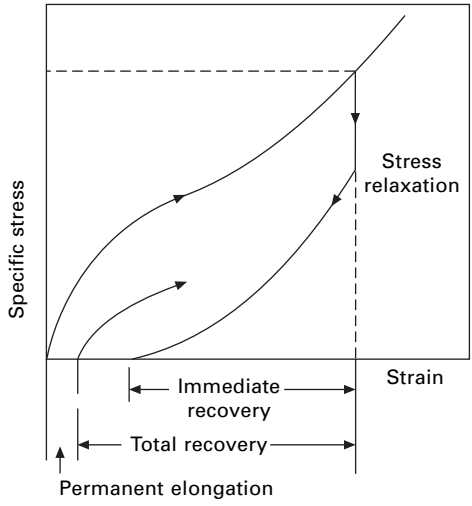

15.5 Test procedure used by Hockenberger *et al*. [2].

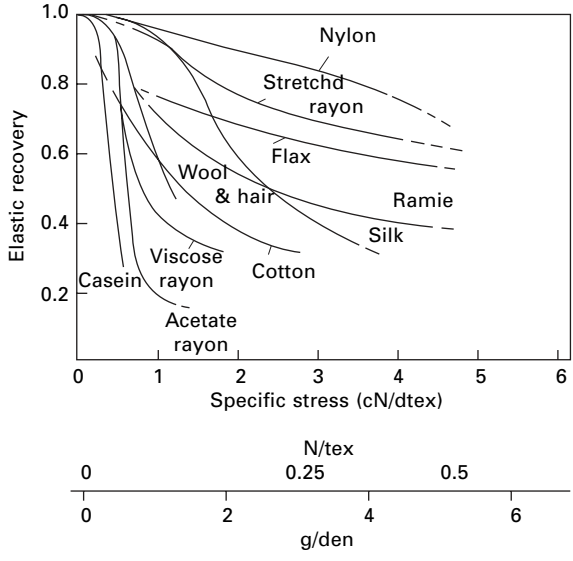

15.6 Elastic recovery plotted against stress. After Meredith [1].

15.4 Results

15.4.1 Comparative values

Elastic recovery may be plotted against stress or strain. The first shows the extent to which a given force will cause permanent damage to a fibre. The second shows what proportion of a given extension will be recovered and the amount of the permanent deformation. Figs 15.6 and 15.7 show Meredith's results.

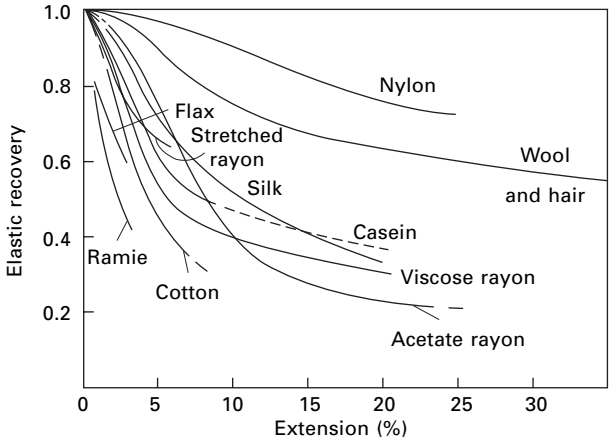

15.7 Elastic recovery plotted against strain. After Meredith [1].

In cotton, the elastic recovery from a given strain is almost independent of the variety, but, since coarse cottons have a lower modulus, it follows that they will show less recovery from a given stress. Cotton shows no yield point (or it may be more correct to say that the yield point is at zero stress and zero strain). The elastic recovery falls steadily to about 0.3. Compared with that of other fibres, the recovery of cotton is only moderate. In particular, even small strains leave an appreciable proportion of permanent deformation.

The bast fibres show poor recovery from strain but can withstand large stress without great permanent damage.

Viscose rayon and acetate show a marked yield point. Below this point, the recovery is good, but above it the curve drops rapidly, and the recovery is poor. The stretched rayons can stand higher stresses without suffering permanent deformation.

Wool and hair also show a yield point, but the drop in the curve is less rapid, and even near break there is still considerable recovery. These fibres are not good under high stresses but can recover from large strains. Thus they show 60% recovery from an extension of 35%. By contrast, in the casein fibre tested, the curve drops rapidly above the yield point, and the large additional extension that can occur before break is almost entirely non-recoverable. Thus, though the stress–strain curves of wool and casein are similar, their recovery behaviour is quite different, and this is one of the reasons why the regenerated-protein fibres of the 1950s did not last.

Wet wool fibres show complete recovery up to the end of the yield region (30% extension) and very good recovery from higher strains. However, the path of the recovery curve is different from that of the extension curve, as shown in Fig. 15.8, and thus there is energy loss in cyclic deformation.

Silk shows fairly good elastic recovery from both stress and strain.

Nylon shows the best elastic recovery of any of the fibres tested by Meredith, whether considered on the basis of stress or on that of strain. Even near break, its recovery falls only to 0.7. Although, in strength and extension at break, nylon is surpassed by some other fibres, these curves show its superiority in resisting permanent damage as a result of undue stress or strain.

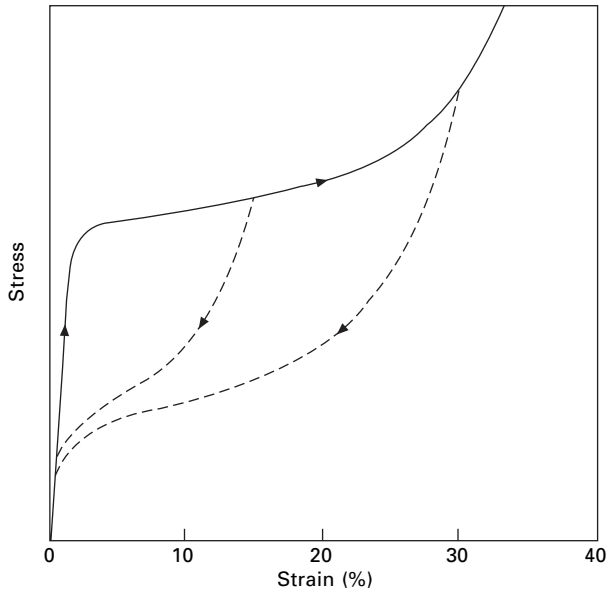

15.8 Stress–strain behaviour of wool in extension and recovery. The stress is in arbitrary units.

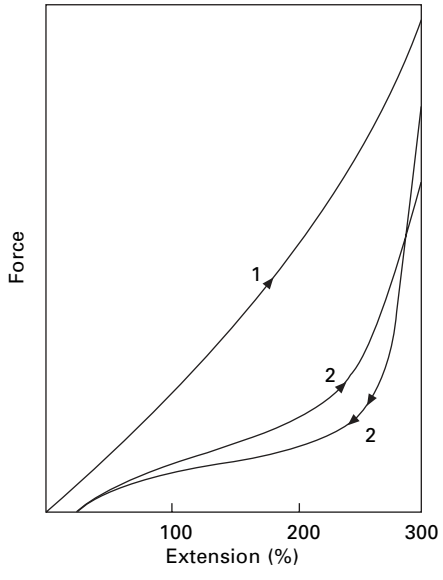

15.9 Cycling response of spandex fibre: 1, first elongation; 2, 6th cycle loading and unloading [3].

After some time on a package, spandex fibres such as *Lycra* acquire a temporary set, and the first elongation shows a high stiffness. As shown in Fig. 15.9, a small amount of the initial extension is not recovered; in subsequent elongations, a steady hysteresis cycle with good reversible behaviour is established [3].

It is interesting to compare values of the yield point obtained from stress–strain curves (see Section 13.5) with those from recovery curves (arbitrarily defined as the point of 95% recovery). This is done in Table 15.1. It will be seen that there is qualitative agreement, though the values from the stress–strain curves are generally higher than those from the recovery curves.

Beste and Hoffman [4] measured the elastic recovery of fibres, by means of a slightly different experimental procedure, and obtained results in general agreement with those of Meredith. They made tests at relative humidities of 60 and 90%, and examples of their results are given in Table 15.2. It will be seen that at small strains the elastic recovery is less at the higher humidity, but at larger strains it is greater for a number of the materials. They also measured work recovery, and some of their results are shown in Fig. 15.10. This shows that, at large strains, the energy dissipated by nylon is considerably less than that by other fibres.

Table 15.1 Yield point

Fibre	From-stress-strain curves		From recovery curves	
	Stress (mN/tex)	Strain (%)	Stress (mN/tex)	Strain (%)
Cotton	–	–	9	1
Viscose rayon	59	2	39	1
Acetate	69	3	39	2
Stretched rayon	118	0.8	88	1
Wool	59	5	39	4
Casein	49	5	29	1
Silk	156	3.3	98	4
Nylon	402	16	127	8

Table 15.2 Effect of humidity on elastic recovery [4]

Material	Elastic recovery (%) from:					
	1% extension		5% extension		10% extension	
	60% r.h.	90% r.h.	60% r.h.	90% r.h.	60% r.h.	90% r.h.
Cotton	91	83	52	59	–	–
Viscose rayon	67	60	32	28	23	27
Acetate	96	75	46	37	24	22
Wool	99	94	69	82	51	56
Silk	84	78	52	58	34	45
Nylon	90	92	89	90	89	–
Polyethylene terephthalate (Dacron)	98	92	65	60	51	47
Polyacrylonitrile (Orlon)	92	90	50	48	43	39
Casein	90	76	47	43	30	25

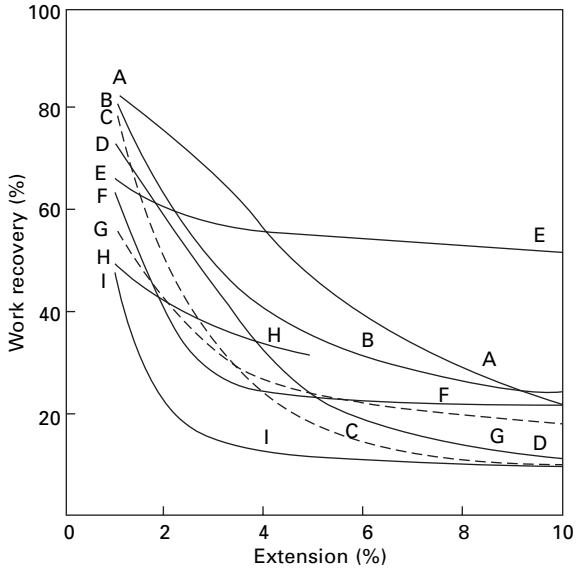

15.10 Work recovery of fibres After Beste and Hoffman [4]: A, wool; B, Dacron polyester fibre; C, acetate; D, casein; E, nylon; F, Orlon acrylic fibre; G, silk; H, cotton; I viscose rayon.

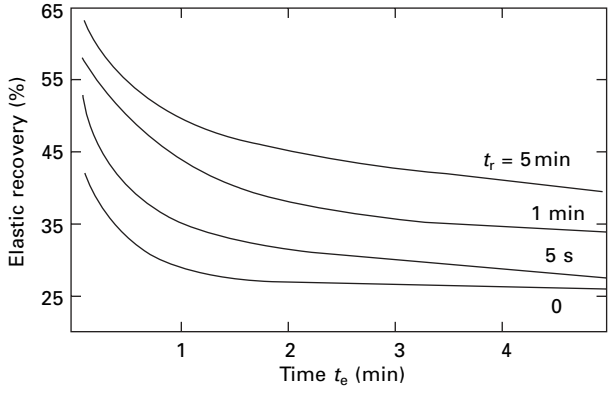

15.11 Elastic recovery of viscose rayon, showing variation with time extended, t_e, and recovery time, t_r.

15.4.2 Influence of test conditions on recovery

Values obtained for elastic recovery are very sensitive to conditions. Guthrie and Norman [5] studied the influence of the time t_e for which viscose rayon fibres were held at constant strain and the time t_r of recovery at zero stress. The rate of extension and contraction was 100%/min. Figure 15.11 shows their results and indicates that any value between 25 and 65% could be obtained, depending on the test procedure. Even if, as is often done, the two times were made equal, the values would range

from 50 to 38%. Similar behaviour in other fibres has been described by Guthrie and Wibberley [6], and the problem has also been discussed by Hadley [7].

Temperature will also influence recovery behaviour, as described for acrylic fibres by Beevers and Heap [8]. Ford [9] lists the elastic recoveries, wet and dry, at 20 °C and 95 °C, for many types of fibre. Figure 15.12 shows values for continuous filament nylon 66 and polyester fibres, both of which have tenacities of about 0.45 N tex and breaking extensions of 20%. Polyester fibres show better recovery than nylon at low stresses, but fall off more at high stresses. For glass fibres the elastic recovery was 85% for all conditions and strains.

A comparative set of work recovery values from a comprehensive study of recovery reported by du Pont [10] is given in Table 15.3. The comparatively poor work recovery of nylon is due to 'creep' and 'creep recovery', which leads to substantial hysteresis. Polyester shows better recovery from small strains than nylon, but poorer from large strains.

15.5 Change of properties as a result of straining: mechanical conditioning

Stretching a fibre far enough to leave it with a permanent set causes other changes in the properties of the fibre. This is illustrated in the idealised model of Fig. 15.13. When the fibre is first strained, the stress–strain curve OA is followed, but, on removal of the load, recovery takes place along AB, the permanent extension OB being left. If the fibre is again stressed, the curve BAC is followed. Re-plotting this as a new stress–strain curve (Fig 15.13(b)), we see that the effect of the first straining has been to raise the yield stress and reduce the breaking extension (and consequently the work of rupture). This has practical implications, since it means that the properties of fibres may be changed by high forces during processing. It also means that if a structure is highly strained in use, even though it is not broken, its properties will be altered, and it may no longer serve its proper function.

The rise in the yield stress means that the application of a given stress to a fibre for some time usually results in almost perfect recovery from subsequent stresses below this value. This treatment is known as mechanical conditioning. Table 15.4 gives values of elastic recovery from near the breaking point before and after mechanical conditioning at 80% of the breaking elongation. It will be seen that there is little permanent deformation in the tests after mechanical conditioning, even though this is taken to a greater extension.

Averett *et al*. [12] studied a partially oriented nylon fibre (draw ratio of 2.5×), which shows a large plastic extension beyond the yield point. Figure 15.14 shows its response to cyclic loading at increasing loads. The initial modulus is appreciably lower than in the initial elongation. Figure 15.15 shows the division between elastic and plastic extension.

If a fibre is repeatedly taken through a given cycle of stress, the loading and unloading curves in successive cycles will gradually come closer together until they form a continuously repeated loop. This is illustrated in Fig. 15.16. The area within the loop will be a measure of the energy dissipated in each cycle.

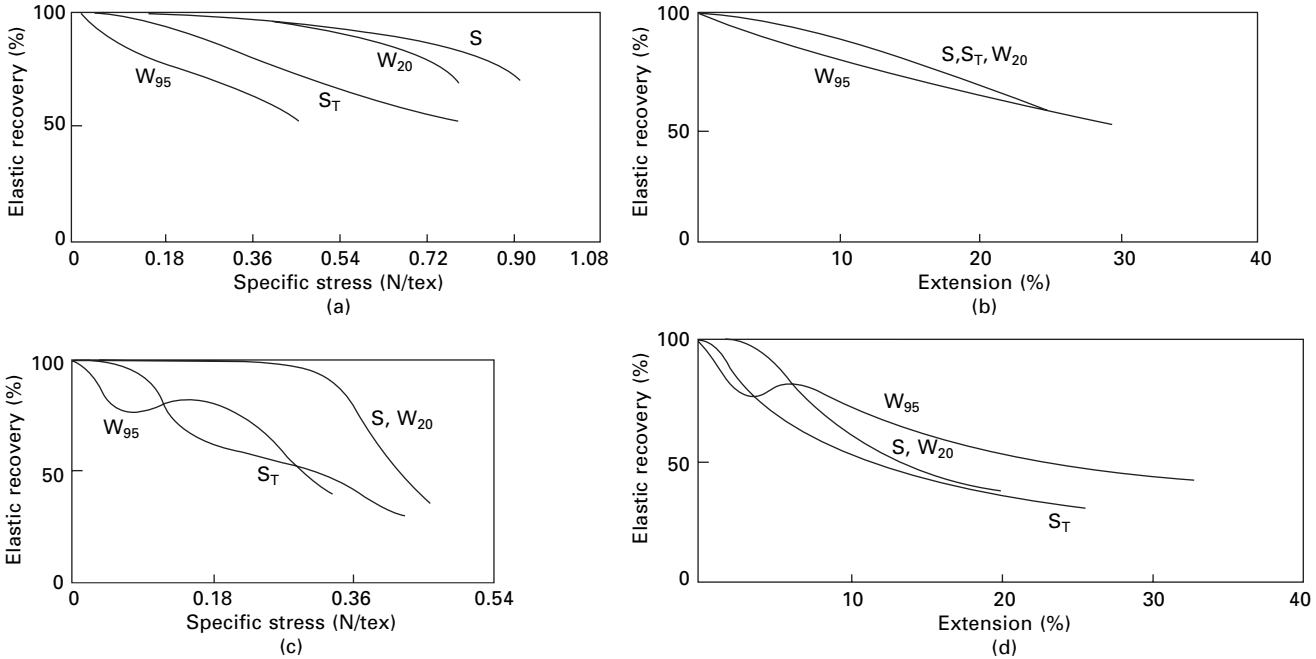

15.12 Elastic recovery under various conditions. S, as received tested at 65% r.h., 20 °C; S_T, 65% r.h., 20 °C after water at 95 °C; W_{20}, in water at 20 °C; W_{95}, in water at 95 °C: (a), (b) nylon 66; (c), (d) polyester. (a) and (c) From given stress; (b) and (d) from given strain.

Table 15.3 Percentage work-recovery values [10]

	Acetate	Polyester fibre	Nylon	Acrylic fibre	Rayon	Wool
From 1% extension	60	81	51	55	32	80
3% extension	32	34	42	28	18	43
5% extension	17	22	47	14	13	27
15% extension	7	19	43	10	11	15
At 8% r.h	42	38	38	31	22	50
92% r.h.	21	28	78	26	16	58
In water at 21 °C	20	41	73	22	58	43
76 °C	7	21	95	13 at 50 °C	80	61
In air at – 70 °C	55	57	45	56	25	68
177 °C	5	33	54	29	12	25
After holding 1 s	47	49	60	40	27	66
900 s	13	23	24	10	8	25

Standard conditions (except as indicated above): 21 °C, 65% r.h.; 3% extension; 30 s holding time.

Cotton had a work recover of 67% under standard conditions.

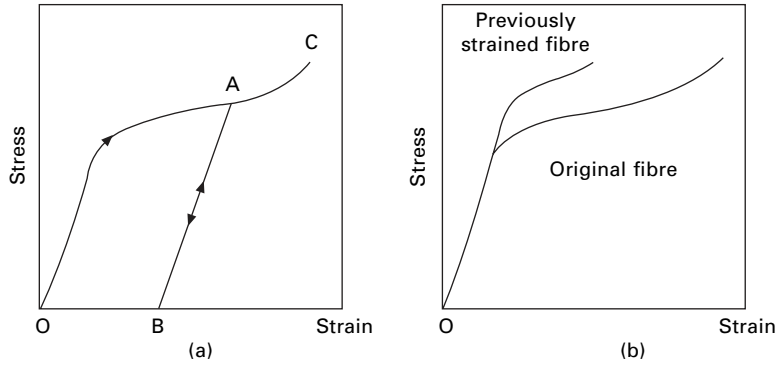

15.13 Change in fibre properties on straining.

15.6 Swelling recovery

For fibres that absorb water, the 'permanent' (plastic) extension as defined in Figs 15.3 and 15.5 is partly recovered on immersion in water or treatment in steam. The fibre will revert almost to its original form on subsequent drying. When a fibre is wetted, it usually extends owing to swelling, but the swelling recovery may cause a net contraction. Swelling recovery may be useful as a means of restoring the original fibre properties, but it also means that fibres that have been stretched in processing will shrink on wetting. Table 15.5 shows values of swelling recovery obtained by Leaderman [14]. Viscose rayon shows almost complete recovery in water, as does silk in steam, but acetate shows only partial recovery.

Immersion of 'permanently' strained wool fibres in water for 24 hours serves to restore their properties to a standard state. This procedure was used by Feughelman [15] to make repeated tests on the same wool fibres.

Table 15.4 Effect of mechanical conditioning on elastic recovery [11]

Material	Elastic recovery % near breaking point	
	Before mechanical Conditioning	After mechanical conditioning
Cotton yarn	56	80
Fortisan (stretched cellulose)	72	94
Acetate	30	92
Silk	36	93
Viscose rayon	39	74
Dacron polyester fibre	55	92
Orlon acrylic fibre	58	92
Vicara (zein protein)	43	97
Casein	39	80
Nylon	72	92
Wool	59	88

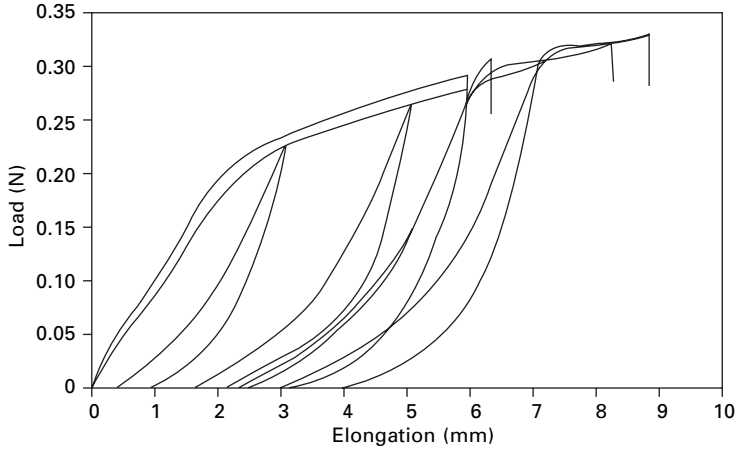

15.14 Cyclic responses of a partially orientated, 33 μm diameter nylon fibre at increasing loads. Gauge length of 25.4 mm means that 10 mm elongation = 40% extension. From Averett *et al.* [12].

15.7 Simple recovery models

15.7.1 Idealised fibre stress–strain relations

In dealing with other materials, ideal elasticity (Hooke's Law) or ideal plasticity (a Hooke's Law region leading to a constant plastic-yield stress) is often assumed. Neither of these is very suitable for representing fibre behaviour. Instead, a form that gives a reasonable approximation to the behaviour of many fibres is shown in Fig. 15.17. It is often helpful to use this form in studying the response of fibres to complicated loading sequences, though some fibres, of which wool is a notable example, deviate markedly from the idealised behaviour. The idealised model is characterised by four parameters: two slopes, yield strain and breaking strain.

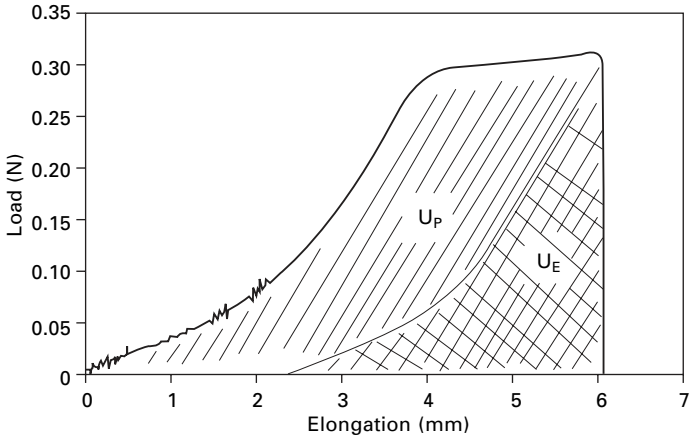

15.15 Elastic energy U_E and plastic energy U_P after load-cycling for the partially oriented nylon fibre. From Averett *et al.* [12].

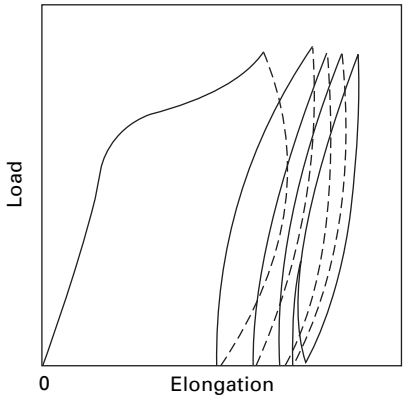

15.16 Load – elongation curves for acetate under repeated stressing to 90% of breaking load. After Hamburger [13].

Table 15.5 Swelling recovery [14]

Material	Permanent extension (%)	Permanent extension (%) after recovery in:	
		Water	Steam
Viscose rayon	1.7	0.08	–
Silk	1.2	0.7	(–0.02)
Acetate	4.1	3.3	1.6

15.7.2 Recovery, work of rupture and durability

In use, fibres are frequently subjected to shocks of given energy, well below their work of rupture. Failure does not occur initially, but a succession of repeated shocks can lead up the stress–strain curve to the point of break, as shown in Fig. 15.18.

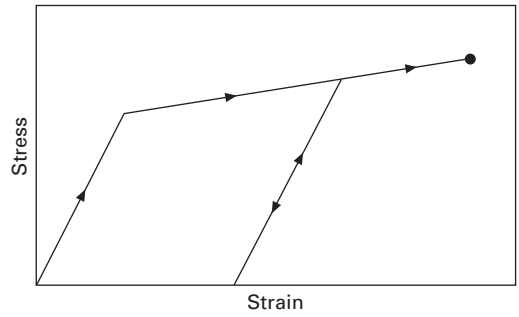

15.17 Simple idealised fibre stress–strain curve.

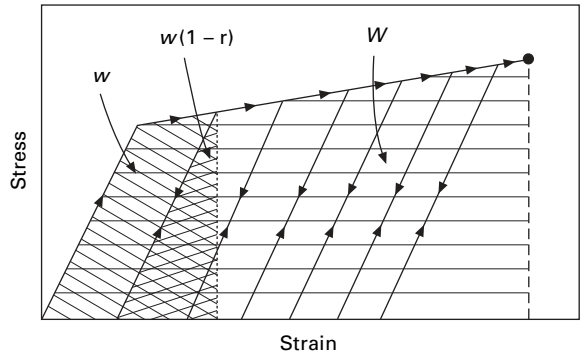

15.18 Behaviour of idealised fibre subject to repeated shocks of energy (w).

If the imposed shock has an energy w, and if the work recovery in a given cycle is r, then the amount of energy used up in the cycle is $w(1 - r)$. If the additional elastic energy in the final cycle is ignored, it follows that failure will occur when the total energy used up equals the work of rupture W of the fibre. This means that the life of the fibres, expressed in terms of the number N of shocks that it will resist, is given by:

$$\sum_{1}^{N} w(1 - r) = W \tag{15.1}$$

If, to show up the nature of the relation more clearly, we take w and r as constants, we find that:

$$N = \frac{W}{(1 - r)w} \tag{15.2}$$

Long life therefore results, rather obviously, from gentle use, giving a low value of w, and more importantly, from the use of fibres with high work of rupture W and good recovery properties, namely, values of r close to 1.

15.7.3 A simple model of cyclic testing

Hearle and Plonsker [16] have explained some of the features of cumulative-extension and other forms of cyclic testing on the basis of a simple model of recovery behaviour

with the essential features shown in the stress–strain curve, Fig. 15.19, which is not quite as restricted as Fig. 15.17. The assumptions are as follows:

- The stress–strain curve in simple extension is ABE. If a specimen is strained to any point B and allowed to recover to C, it is assumed that, on re-straining, the original stress–strain curve will be rejoined at B and then followed towards E.
- It is assumed that, on first reaching any strain level, such as B, the elastic recovery r, defined as the ratio of elastic strain R to total strain ε, will be a function only of strain ε. In particular, r will be independent of the previous history at lower strain levels.

These are the two basic assumptions, but we can add three others, as follows:

- Repeated application of the same level of strain B does not lead to any change in the elastic-recovery value.
- Viscoelastic time-dependent effects are ignored.
- Break occurs at the same point E irrespective of the previous history, so that any true 'fatigue' effects are not taken into account.

We can now note the behaviour in simple cycling procedures. Simple extension-cycling between fixed limits of imposed strain without the removal of slack is shown in Fig. 15.20(a). Initially, the stress–strain curve is followed from A to B; recovery to zero strain goes along BCA; and then re-straining to B reverses the path ACB. The strain level B cannot be exceeded, and the path BCACB is followed in all succeeding cycles. It will be noted that the return path from C to B has been shown here as different from the path from B to C: this, while it is avoided in the simpler model shown in Figure 15.19, is not incompatible with the basic assumptions.

Simple load-cycling, as in Figure 15.20(b) between the levels A and B, is almost identical, except that there is an immediate reversal at C, without traversing the region of slack fibre back to the original length at A.

Figure 15.21 illustrates the behaviour of the basic model in cumulative-extension cycling. An imposed strain ε_1 is applied to the material and then released; the material

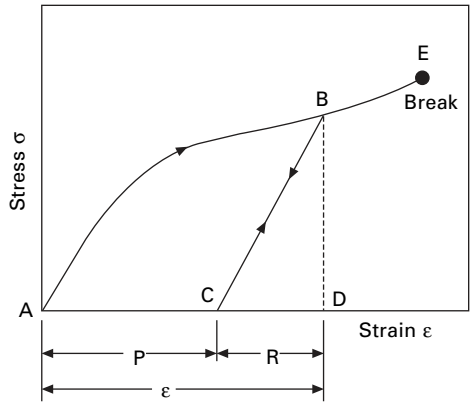

15.19 Idealised model of recovery behaviour.

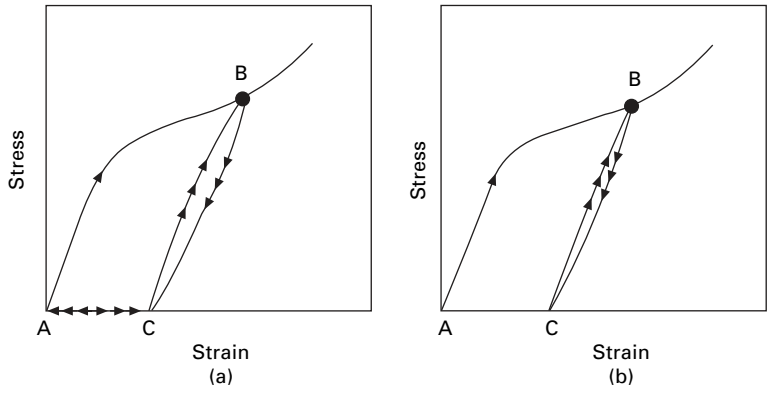

15.20 Model in (a) simple extension-cycling and (b) load-cycling.

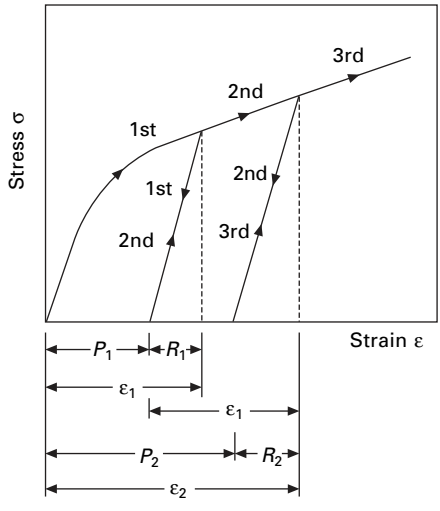

15.21 Model in cumulative extension-cycling.

has a permanent strain P_1 after this first cycle. The slack P_1 is removed, and then the imposed strain ε_1 is again applied. The strain on the material in the second cycle is now $\varepsilon_2 = P_1 + \varepsilon_1$; after the second cycle, the permanent strain is P_2, and this is removed before applying ε_1; and so on. The gradual increase of strain is given by noting that, in the $(n - 1)$th cycle:

$$\text{permanent strain} = P_{n-1} = (1 - r_{n-1})\varepsilon_{n-1} \tag{15.3}$$

in the nth cycle:

$$\text{total strain} = \varepsilon_n = P_{n-1} + \varepsilon_1 = (1 - r_{n-1})\,\varepsilon_{n-1} + \varepsilon_1 \tag{15.4}$$

$$\text{permanent strain} = (1 - r_n)\,\varepsilon_n \tag{15.5}$$

in the $(n + 1)$th cycle:

$$\text{total strain} = \varepsilon_{n+1} = P_n + \varepsilon_1 = (1 - r_n)\,\varepsilon_n + \varepsilon_1 \tag{15.6}$$

The strain will have reached a limiting value when the total strain in successive cycles remains unaltered, that is, when:

$$\varepsilon_n = \varepsilon_{n+1} \tag{15.7}$$

$$\varepsilon_n = (1 - r_n)\,\varepsilon_n + \varepsilon_1 \tag{15.8}$$

$$\varepsilon_n r_n = \varepsilon_1 \tag{15.9}$$

In general, the condition for the limiting extension is thus:

$$\varepsilon r = \varepsilon_1 \tag{15.10}$$

where ε_1 is the constant strain imposed in each cycle. This condition states that, at the limit, the strain recovered after a cycle just equals the imposed strain, so that there is no additional straining in the next cycle.

If elastic-recovery values are known as a function of ε_1, then equations (15.3) to (15.6) can be used to compute the total elastic and permanent strains in each successive cycle.

Three different types of behaviour are predicted during cumulative extension cycling: (1) if the limiting extension is less than the breaking extension, the specimen will steadily increase in length until it reaches the stable limiting value; (2) if the limiting extension is greater than the breaking extension, the specimen will fail before it reaches the limit; and (3) there may be no limiting extension, and hence the specimen will extend indefinitely and finally fail by breaking. The distinction between (2) and (3) is, in a way, artificial, since both describe a steady increase in extension up to the breaking point. However, in some instances, extrapolated recovery curves would lead to a limit, whereas in other instances they lead away from a limit. In using the recovery values for nylon, there is a rather sharp change at a level of imposed extension of 10.7% from a stable limit to an indefinite increase in length.

15.7.4 Experimental behaviour in cyclic testing

For comparison with the predictions given in Fig. 15.20, Fig. 15.22 shows the behaviour of an acetate fibre in simple extension and load cycling. Contrary to the behaviour of

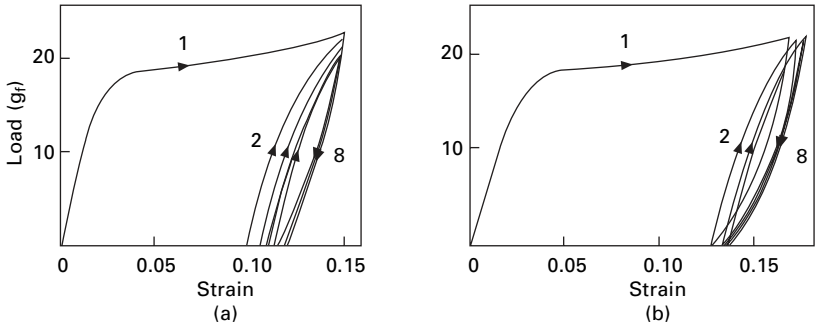

15.22 Behaviour of 2.5 tex acetate in (a) simple extension-cycling and (b) load-cycling.

the model, there is a gradual reduction of peak stress and increase of permanent extension (decrease of elastic recovery) in successive cycles of simple extension cycling; and there is a corresponding increase of total and permanent extension in load cycling. These effects correspond to the occurrence of some secondary creep (non-recoverable time-dependent extension) as the test proceeds.

In cumulative-extension cycling, the experimental results as illustrated in Fig. 15.23 for acetate and nylon do show that, at low imposed strains, a limiting extension is reached, whereas at high imposed strains the extension continues until break occurs. The computed values based on recovery values predict appreciably less permanent extension than is observed in practice, which is due to deviation of the behaviour of real fibres from that of the simple model. Time-dependent aspects of cumulative-extension are discussed in Section 16.2.5 and in relation to fatigue in Section 19.3.

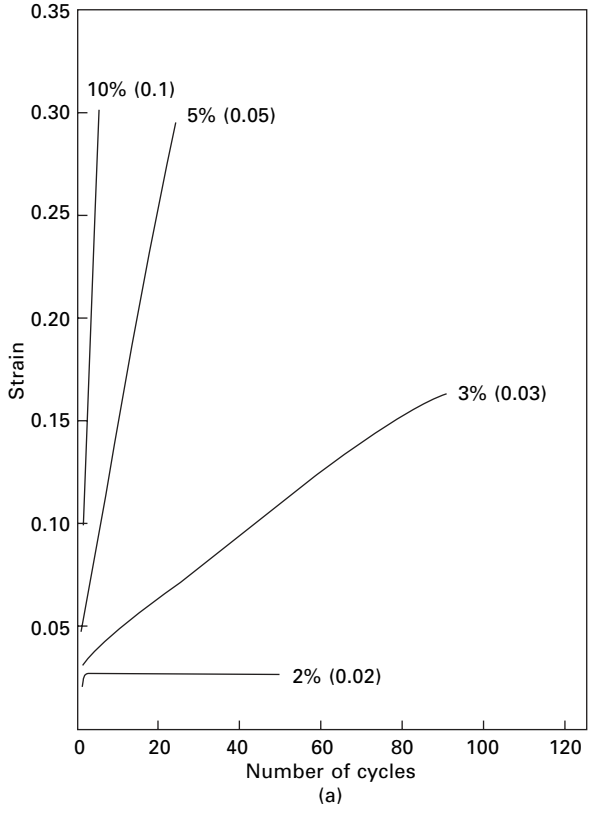

15.23 Behaviour of (a) acetate and (b) nylon at various levels of imposed extension in cumulative-extension tests.

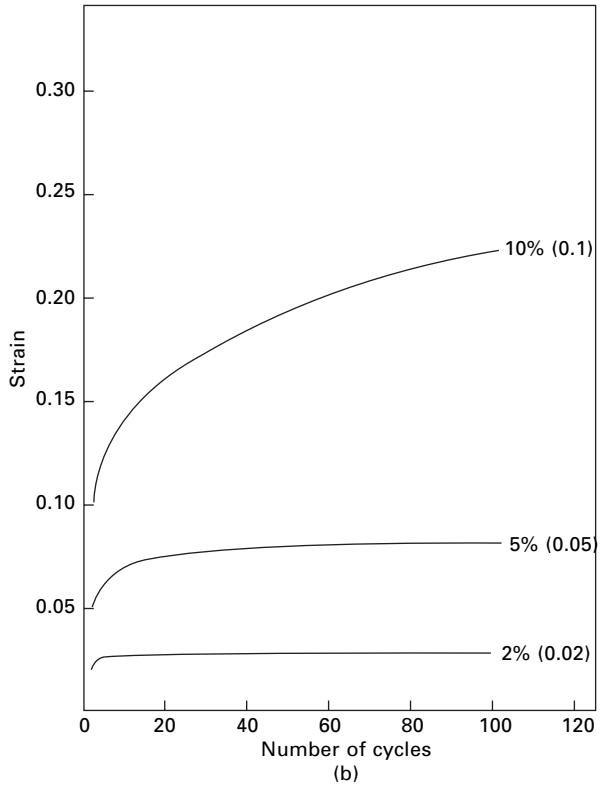

15.23 (Continued)

15.8 References

1. R. Meredith. *J. Text. Inst.*, 1945, **36**, T147.
2. A. R. Hockenberger, S. Koral and M. A. Wilding. *Textile Res. J.*, 2005, **75**, 111.
3. A. J. Hughes and J. E. McIntyre (Coordinators). *Textile Progress*, 1976, **8**, No. l.
4. L. F. Beste and R. M. Hoffman. *Text. Res. J.*, 1950, **20**, 441.
5. J. C. Guthrie and S. Norman. *J. Text. Inst.*, 1961, **52**, T503.
6. J. C. Guthrie and J. Wibberley. *J. Text. Inst.*, 1965, **56**, T97.
7. D. W. Hadley. *J. Text. Inst.*, 1969, **60**, 301, 312.
8. R. B. Beevers and S. A. Heap. *J. Text. Inst.*, 1966, **57**, T191.
9. J. E. Ford (Editor). *Fibre Data Summaries*, Shirley Institute, Manchester, 1966.
10. Bulletin X–142, E. I. du Pont de Nemours & Co. Inc., Wilmington, DE, 1961.
11. L. Susich, *Text. Res. J.*, 1953, **23**, 545.
12. R. D. Averett, M. L. Realff, S. Michielsen and R. W. Neu. *Composites Sci. Tech.*, 2006, **66**, 1671.
13. W. J. Hamburger. *Text. Res. J.*, 1948, **18**, 102.
14. H. Leaderman. *Elastic and Creep Properties of Filamentous Materials and Other High Polymers*, The Textile Foundation, Washington, DC, 1943, p. 128.
15. M. Feughelman. *Mechanical Properties and Structure of alpha-Keratin Fibres*, UNSW Press, Sydney, 1997.
16. J. W. S. Hearle and H. R. Plonsker. *J. Appl. Polymer Sci.*, 1966, **10**, 1949.

16
Rheology

16.1 The study of time dependence

So far, we have been discussing the mechanical properties of fibres, with only a brief mention of one of the main characters: time. The extension caused by a given applied force, or the stress resulting from a given strain in the fibre, depends on how long the force or the strain has been present and on the earlier mechanical history of the fibre.

On the application of a load to a fibre, it will, after an instantaneous extension, continue to extend as time goes on. On removal of the load, the recovery will not be limited to the instantaneous recovery but will continue to take place. This behaviour is illustrated in Fig. 16.1(a) and is known as creep and creep recovery. It may continue for a very long time, as illustrated in Fig. 16.2. Creep is extension with time under an applied load: the complementary effect is stress relaxation, the reduction of tension with time under a given extension. This is illustrated in Fig. 16.1(b): when the fibre is stretched, an instantaneous stress is set up, but this gradually decreases as time passes.

The continued deformation and possible rupture of the specimen when a load is applied for some time have important consequences in the testing of mechanical

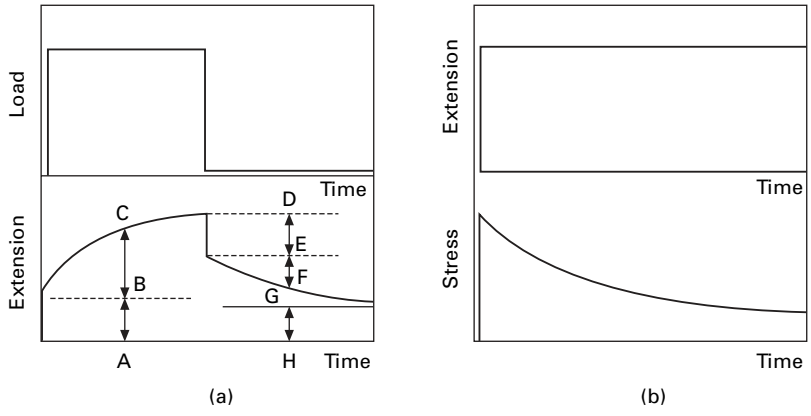

16.1 (a) Creep under constant load and recovery under zero load, showing instantaneous extension, A–B and D–E; total creep, B–C; primary creep, E–F; and secondary creep, G–H. (b) Relaxation of stress under constant extension.

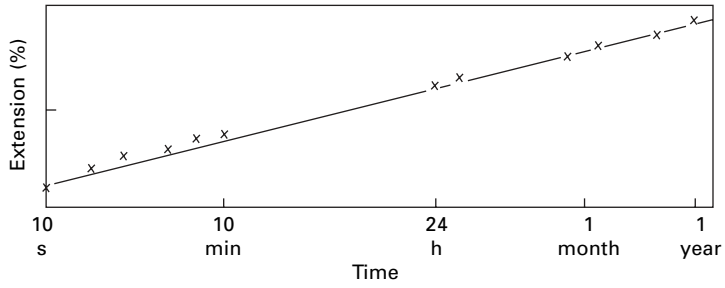

16.2 Creep of 16.5 den (1.8 tex) nylon under a load of 30 gf (0.29 N) continuing for one year [1].

properties, since it means that the results of a test, for example the stress–strain curve obtained, will depend on the timing. This in turn creates interest in the high-speed properties of fibres, the study of which needs special experimental techniques, since conventional methods of testing have time-scales that cannot be shorter than a few seconds. With very rapid tests, there is the further complication that they may be more nearly adiabatic than isothermal.

An alternative means of studying time dependence is to subject the fibre to an oscillating load: dynamic testing.

The four methods suggested are the simplest of the infinite variety of time sequences of stress and strain that a fibre might experience. Between them, they conveniently cover a wide range of times. The timescales for which the methods are easily used are as follows:

- creep: long times, from 1 minute to 1 month
- stress relaxation: medium to long times, from 1 second to 1 hour
- stress–strain curves, including impact methods: short to medium times, from 1/100 second to 10 minutes
- dynamic testing: short times, from 0.1 millisecond to 1 second.

These time ranges can be increased somewhat by more elaborate or difficult experimental methods.

Effects in the processing or use of fibres are liable to cover all the time ranges and to involve more complicated variations of stress and strain with time. One aim of the development of the academic subject of fibre rheology should be to provide means of predicting behaviour in real situations.

16.2 Creep

16.2.1 Primary and secondary creep

Figure 16.1(a) indicates the effect of applying a constant load to a fibre for a given time and then removing it. The instantaneous extension is followed by creep. The removal of load gives rise to an instantaneous recovery, usually equal to the instantaneous extension, followed by a further partial recovery with time, which still leaves some unrecovered extension. The total extension may therefore be divided into three parts:

the *immediate elastic deformation*, which is instantaneous and recoverable; the *primary creep*, which is recoverable in time; and the secondary creep, which is non-recoverable. The mechanisms of creep will be discussed in Chapter 20, but it is worth noting here that there are two main effects. At low stress, creep is due to localised molecular rearrangement, which may or may not be recoverable. At high stress, molecules slide past one another in non-recoverable deformation.

O'Shaughnessy [2] has studied the division of the total extension of viscose rayon yarn into its three parts. He measured the creep under a constant load and the recovery after various times of loading. Figure 16.3 gives examples of his results plotted on a logarithmic scale, and it will be seen that the secondary creep continues after the primary creep has ceased.

Figure 16.4 shows results calculated from experiments by Press [3] at longer times. In these experiments, recovery was measured only after the full time for creep, and the division between primary and secondary creep depends on the assumption, derived from the superposition principle (see Section 20.7.7), that the time-dependent part of the recovery curve is identical with the primary creep curve.

If, after recovery, the same load is applied again, the rate of creep is less than that in the first test on the specimen. The primary creep takes place at its initial rate, as before, but the secondary resumes at the rate at which it left off. The mechanical conditioning effect is a special case of this, since it means that if the load has been applied for long enough for the rate of secondary creep to become negligible, then there will not be any appreciable secondary creep in later experiments unless the load is further increased. The recovery will therefore be complete. The use of logarithmic timescales may cause some confusion here. The important practical point in mechanical conditioning is that there should be negligible secondary creep on the timescale of

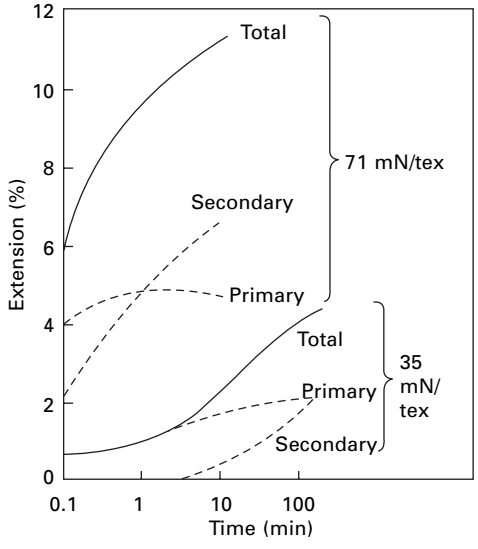

16.3 Primary and secondary creep of viscose rayon at 60% r.h. [2].

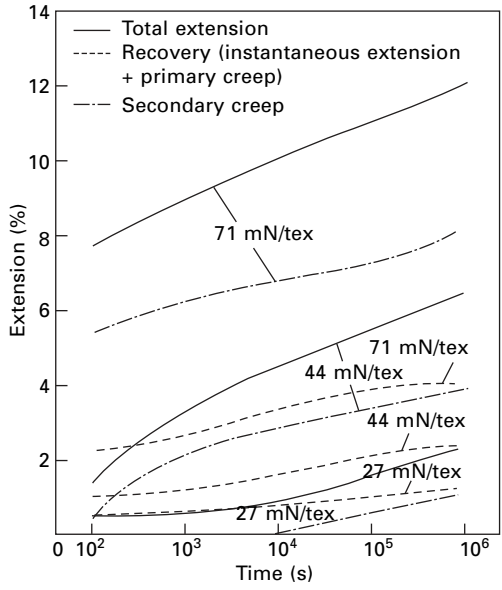

16.4 Creep of viscose rayon at 21 °C, 65% r.h. [3]. 10^2 s ≈ 2 minutes; 10^4 s ≈ 3 hours; 10^6 s ≈ 12 days.

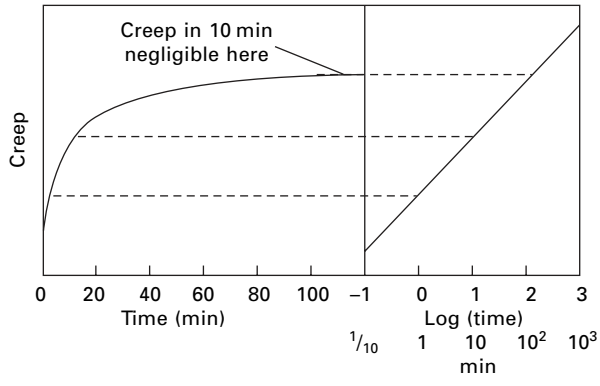

16.5 Comparison of linear and logarithmic timescales.

the experiments; this may be so even when a plot on a logarithmic scale shows that secondary creep has not ceased, and this is illustrated in Fig. 16.5.

The secondary creep gives rise to the major part of the permanent extension of a fibre and is usually negligible below the yield point. Thus a comparison of the amounts of secondary creep that occur in various fibres after particular loading histories is given by the figures for inelastic extension in Chapter 15.

16.2.2 Leaderman's experiments on primary creep

Leaderman [4] carried out a classical investigation of primary creep in viscose rayon, acetate, silk and nylon. In his experiments, 280 mm (11 in.) specimens were mounted

on one arm of a balance. At zero time, the other arm of the balance was released so that a given load was applied to the filament, whose extension was followed by a cathetometer. Measurements were made every 15 seconds for the first minute and thereafter at longer intervals up to 24 hours after the application of the load. Most of Leaderman's tests were made at 65% r.h. and 21 °C, but there were also arrangements for testing dry fibres over a range of temperatures.

To ensure that only primary creep was involved, the stresses employed were small and the specimen was first mechanically conditioned, since it was found that the first application of a load resulted in some permanent deformation but that subsequent applications showed perfect recovery.

When extension is plotted against time, curves such as the one in Fig. 16.6 are obtained. To show the behaviour over a long time, it is more useful to plot the results on a logarithmic scale of time. This is done in Fig. 16.7, which shows the results obtained by Leaderman for various fibres. It is clear from these graphs that the amount of extension occurring as primary creep is comparable to that occurring instantaneously.

In viscose rayon and acetate, the recovery curves are identical with the creep curves inverted, as is shown in Fig. 16.8(b). In silk, the recovery curves are the same shape as the creep curves but lie slightly higher than those in Figure 16.8(b). This means that the instantaneous contraction on removing the load is less than the instantaneous extension found on applying it.

In nylon at low loads, the recovery curve is the same as the creep curve, but at high loads the behaviour is that shown in Fig. 16.8(c). It will be seen that the instantaneous contraction is less than the instantaneous extension, but the rate of recovery is greater than the rate of creep, so that after a long time recovery is complete. The rate of recovery is, in fact, found to be the same for all loads above a certain level.

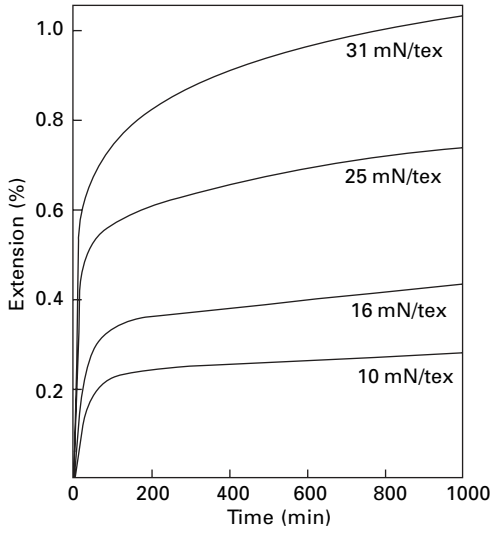

16.6 Primary creep of viscose rayon [4].

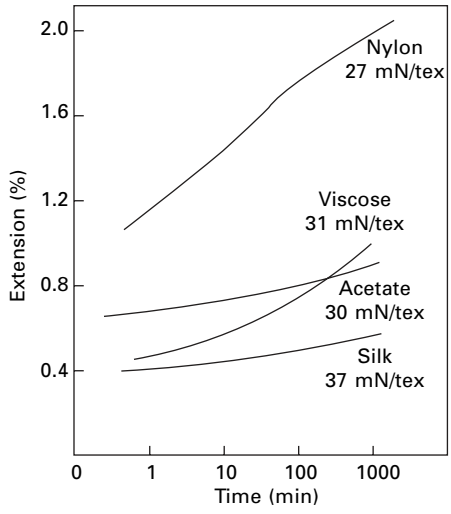

16.7 Primary creep of various fibres [4].

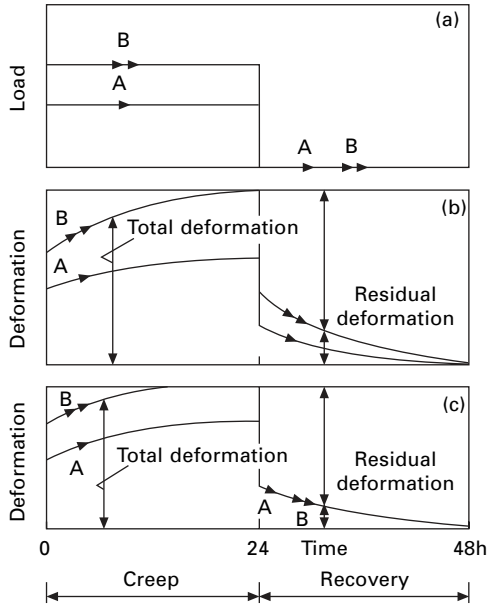

16.8 Creep and recovery of fibres [4]: (a) Load–time diagram; (b) behaviour of viscose rayon and acetate; and of nylon at low loads; (c) behaviour of nylon at high loads.

The shape of the creep curves appears to be different for the different fibres. This is largely a result of the limits on the times for which tests can be made. It is not possible to make measurements at very short time intervals, and it is not practicable to make them at very long time intervals. If this could be done, we should expect all the curves to be sigmoidal, as in Fig. 16.9. It will be seen from this diagram that the

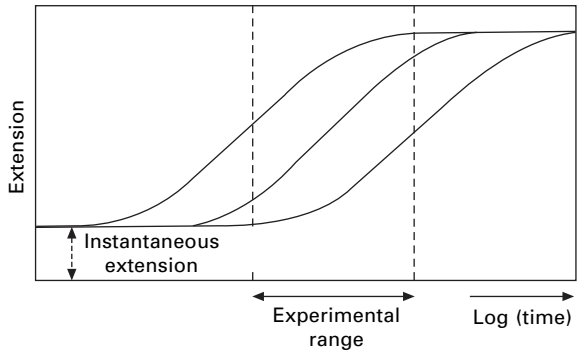

16.9 Creep curves over a wide range of times.

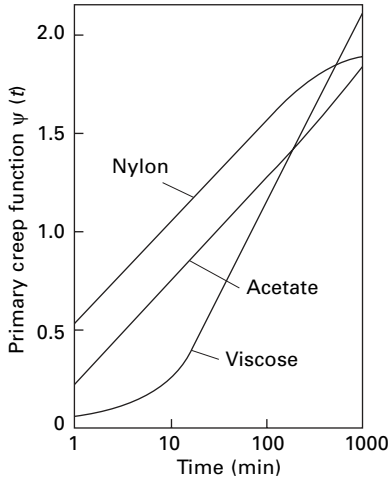

16.10 Values of $\Psi(t)$, calculated from Leaderman's data [4], plotted against time. The value of instantaneous extension has been estimated, so that intercepts of graphs are approximate. Slopes that give creep during a given time interval are correct.

shape of curve found experimentally depends on which portion of the curve lies within the experimental time range. The effect of time may be summarised by a function $\Psi(t)$, which equals the ratio of the primary creep (excluding the instantaneous extension) at a time t to the primary creep occurring between 1 and 90 min under the same load. Values obtained from Leaderman's data are plotted in Fig. 16.10.

The effect of load may be summarised by the quantity $x(90)$, which equals the extension occurring between 1 and 90 min. Values are given in Fig. 16.11, which is analogous to a stress–strain diagram. One notable feature is that for nylon at high loads the amount of creep becomes independent of the load.

It follows from the application of the superposition principle, which is discussed later in Section 20.7.7, and is confirmed by Leaderman's experiments, that the total extension x_t occurring after a time t is then given by:

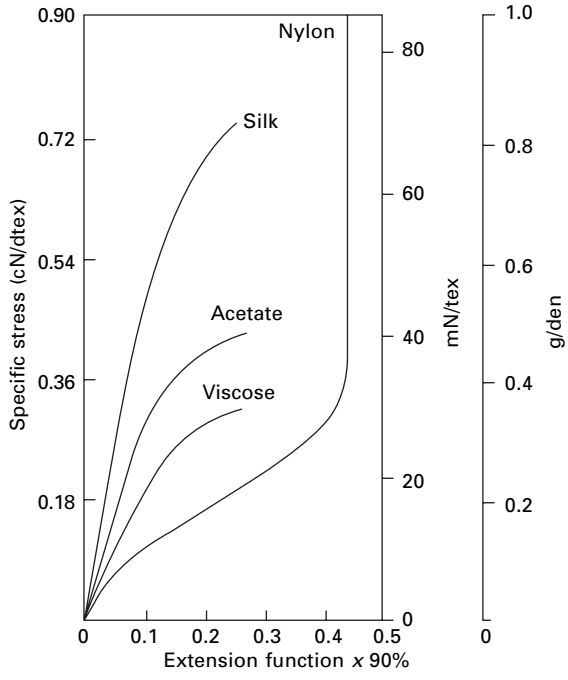

16.11 Values of *x*(90), calculated from Leaderman's data, plotted against stress [4].

$$x_t = x_0 + x(90) \cdot \Psi(t) \tag{16.1}$$

where x_0 = instantaneous extension. This means that, in addition to its special definition (which refers to its absolute magnitude), $x(90)$ gives the relative amount of primary creep at different loads after the same time, in the same way that $\Psi(t)$ gives the relative amount of primary creep at different times under the same load. An interesting result of Leaderman's work, confirmed by many later studies, is the very high level of primary creep in nylon. This has important technical consequences.

16.2.3 Generalised creep curves

O'Shaughnessy [2] showed that the creep of viscose rayon at various loads showed a certain regularity when the elongation divided by the stress was plotted against the time, as shown in Fig. 16.12. It will be seen that, at long and short times, the results for all the loads appear to come together, though for many of the loads this would be at times beyond the experimental range. Thus the creep curves can be regarded as lying between two loci, crossing from one to the other with a characteristic sigmoidal curve (when plotted on a logarithmic time scale) at times that depend on the load.

In a later paper concerned with the creep of nylon, Catsiff *et al*. [5] carried the generalisation of the curves a stage further. The creep curves obtained at various loads, shown in Fig. 16.13, have been fitted to a single master curve by vertical and lateral shift and by multiplying the elongation scale by an appropriate factor. The

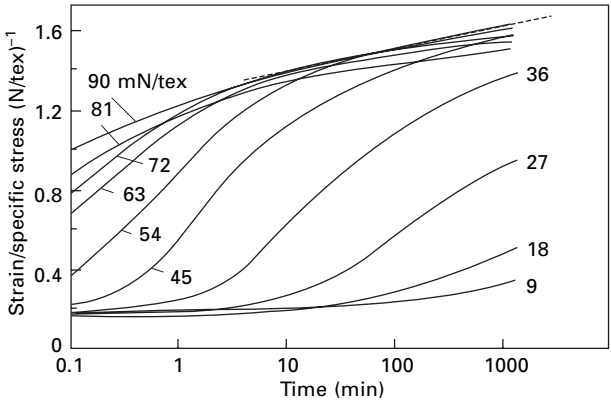

16.12 Generalised creep curves for viscose rayon at 6% r.h. [2].

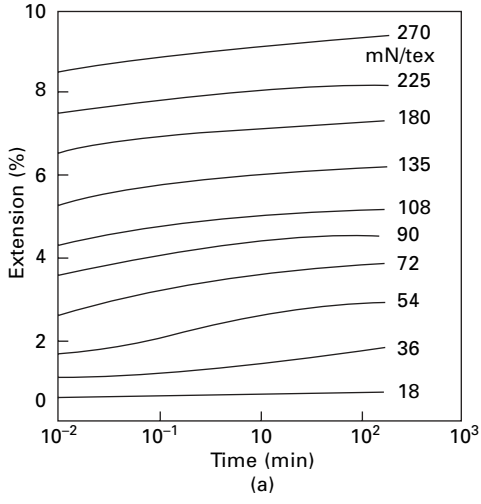

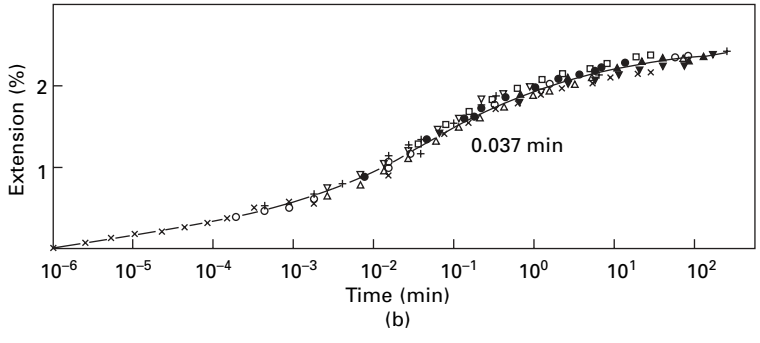

16.13 (a) Creep curves for nylon at 36 °C and 30% r.h.under various stresses [5]. (b) Master creep curve.

experimental results for the various loads group closely round the master curve, and thus, in view of the considerable overlap, it would appear that the agreement is something more than an inevitable result of the procedure for obtaining the master curve.

16.2.4 Influence of various factors on creep

Steinberger [6] found that the creep of acetate increased with the humidity, as is shown in Fig. 16.14. The change was small below 40% r.h. but was considerable at higher humidities. With cuprammonium rayon, Steinberger found that the creep increased at high humidities, but at low humidities he obtained irregular results. Catsiff *et al.* [5] found a similar irregular behaviour in the effect of humidity on the primary and secondary creep of nylon over the whole range of moisture conditions, although the instantaneous elongation increased regularly with humidity.

Leaderman [4] found that the creep of acetate fibre increased as the temperature increased. This was also observed by Feughelman [7], who measured the creep of wool fibres in water at various loads and temperatures, with the results shown in Fig. 16.15. His results were found to fit relations of the form:

$$\frac{1}{\varepsilon_t} = \frac{a}{t} + b \tag{16.2}$$

where ε_t is the strain at time t, and a and b are constants at constant temperature and load.

Ripa and Speakman [8] found a wide variation in creep rates in individual wool fibres, with a few fibres showing an abnormally high rate of creep. A fibre with a high rate of creep follows a normal creep curve for the first 60 min and then turns steeply upwards to give the rapid creep, which suggests that some primary resistance to extension has been broken down. Ripa and Speakman showed that the fibres with a

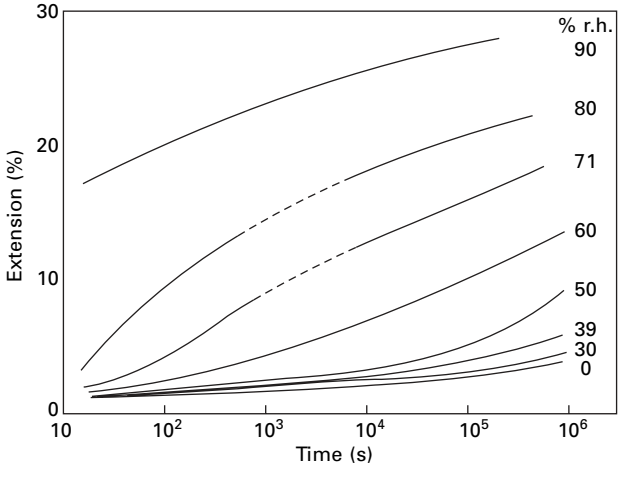

16.14 Effect of humidity on creep of acetate [6].

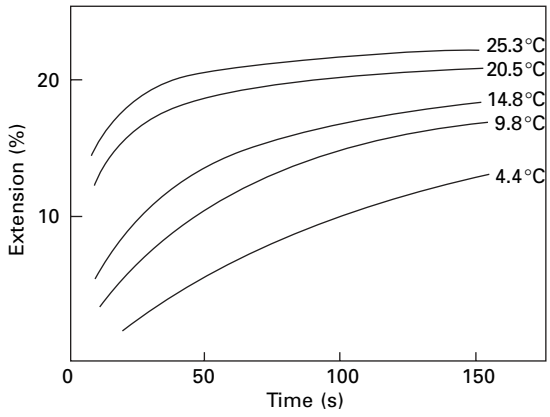

16.15 Effect of temperature on creep of a wool fibre under load of 58.8 mN in water [7].

high rate of creep had a low sulphur content, which suggested that the high rate was associated with a breakdown of cystine crosslinks.

16.2.5 A cumulative-extension test

A set of experiments that involves secondary creep is the cumulative-extension test used by Meredith and Peirce [9]. This test is also interesting as an example of a type involving a cycle of stresses and strains, and to some extent it simulates the repeated loading of fibres in use. This may show up behaviour different from that under a constant or steadily increasing stress or strain. As is indicated in Section 15.7.3, a pure recovery model would indicate a rapid approach either to break or to a limiting extension. The continuing effects are due to the viscoelastic behaviour of the fibre.

The method used was to apply cyclically to the specimen a simple harmonic extension followed by a period of dwell, during which any permanent extension was taken up. The time sequence is shown in Fig. 16.16. The extension was controlled by an eccentric cam and the dwell period with take-up of slack by the release of pawls on a ratchet. Because of the taking-up of the permanent extension, the stress would increase in each cycle, so that mechanical conditioning would not be effective.

The cumulative extension E_n after n cycles was defined by the relation

$$E_n = 100 \log \frac{l_n}{l_0} \tag{16.3}$$

where l_0 = initial length and l_n = length after n cycles. The advantage of this definition is that it is additive, for we have:

$$E_{0\to1} + E_{1\to2} = 100 \left(\log \frac{l_1}{l_0} \right) + \log \frac{l_2}{l_1} = 100 \log \frac{l_2}{l_0} = E_{0\to2} \tag{16.4}$$

For small strains, E_n is approximately equal to the simple strain, $100(l_n - l_0)/l_{0\%}$.

The samples tested were cords of 2000–20 000 den (222–2222 tex). Although they

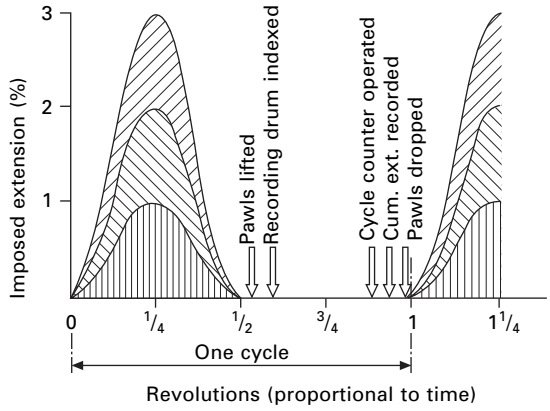

16.16 Time sequence in cumulative-extension test.

were fibre bundles, they indicated comparative fibre behaviour. The tests were made at 65% r.h. and 21 °C. It was found that the residual tension had a considerable effect, since it determined the part of the stress–strain curve at which the test was operating. The standard value used was 10 mN/tex. The cumulative extension decreases as the frequency is increased; the standard tests were made at 1 cycle/second (1 Hz).

In expressing the results, one could give the cumulative-extension (1) after a given number of cycles of a certain imposed extension, (2) after a number of cycles of the same stress pattern, or (3) after the same amount of energy has been imposed in a given number of cycles. Each of these has some significance, and the difference between them is analogous to the difference between breaking extension, breaking load and work of rupture.

Table 16.1 gives examples of the results obtained in these tests. Fibres showing a high value of the cumulative-extension are those which suffer most permanent deformation as a result of repeated straining. Nylon and linen show the least cumulative-extension, though their properties differ in that linen breaks at a lower extension than does nylon. Wool stands up well to extension but extends permanently for large inputs of energy. Casein and viscose rayon show the largest cumulative-extensions.

The type of information given by tests such as this should be added to that given by simpler tests so that a 'personality' for each fibre can be built up.

Some of the fatigue testing described in Chapter 19 has used cumulative-extension testing; the simple recovery aspects of the problem are discussed in Sections 15.7.3 and 15.7.4.

16.2.6 Comparative creep behaviour

Except when cumulative-extension keeps imposing higher strains, creep is comparatively small in cellulosic and protein fibres, except at high loads. In nylon, primary creep is higher. The creep of nylon is also shown when it is used as a matrix in composites [10]. Table 16.2 shows results of tests made on yarns used in high-performance ropes. Polyester and aramid fibres show a small amount of creep. The creep of *Kevlar*

Table 16.1 Cumulative-extension results [9]

Material	Imposed extension of 2%					Cumulative-extension (%) after imposed energy per unit mass of:	
	$E_n - E_1$		Stress in nth cycle (mN/tex)		Cycles to break	0.1 J/g in 100 cycles	1 J/g in 1000 cycles
	n = 10	n = 1000	n = 10	n = 1000			
Cotton	1.98	—	68	—	331	5.2	breaks
Linen	0.66*	—	263	—	75*	1.0	1.1
Viscose rayon	1.79	10..8	51	80	1420	11.7	16.0
Durafil†	1.14	—	177	—	224	1.8	1.9
Acetate	0.35	2.48	37	49	>5000	18.5	breaks
Silk	0.36	1.92	108	144	>5000	1.0	1.6
Nylon	0.28	1.03	51	63	>5000	1.0	1.4
Wool	0.48	1.44	25	29	>2000	5.1	9.2
Casein	1.33	7.12	21	26	>2000	breaks	breaks

*Imposed extension of $1^1/_2$%.
†Lilienfeld rayon, from 1948.

Table 16.2 Creep in one decade of log-time as quoted in *Deepwater Moorings: An* Engineer's Guide, TTI and Noble Denton [11]

	15% break load		30% break load	
	1–10 days	10–100 days	1–10 days	10–100 days
Polyester				
Diolen 855TN	0.240%	0.166%	0.093%	0.034%
Trevira 785	0.119%	0.069%	0.165%	0.009%
Aramid				
Kevlar 29	0.023%	0.066%	0.046%	0.021%
Kevlar 49	0.011%	0.030%	0.041%	0.009%
HMPE				
Spectra 900	1.7% 7/182 days*	13%	broken 0.7/4 days*	broken
Spectra 1000	1.1% 11/321 days*	6.3%	8% 1/28 days*	broken
Dyneema SK60	0.16% 70/>354 days*	0.47%	0.98% 7/123 days*	8%

*The figures in days for HMPE fibres are (time to start of rapid creep)/(time to break).

is due to the removal of misorientation at low stresses. Other liquid-crystal fibres, *Vectran* (melt-spun aromatic copolyester), PBO and M5, have little or no creep. Creep of HMPE fibres is covered in the next section.

16.2.7 Creep of high-modulus polyethylene (HMPE) fibres

The high creep of HMPE is a factor that has to be taken into account in using the fibre. It is not a problem for ballistic protection but would be for mooring oil-rigs for

long periods. The amount of creep varies with the type of HMPE fibre. The first commercial HMPE fibre, *Spectra* 900, had very severe creep as shown in Table 16.2. Adoption of a second heat treatment under tension in *Spectra* 1000 and *Dyneema* SK60 reduced the creep, and it was further reduced in *Dyneema* SK65 and SK75. Alternatively *Dyneema* SK76 is optimised for ballistic protection with high energy absorption.

Extensive studies of creep of HMPE fibres have been reported by Govaert [12] and Jacobs [13]. The creep follows three regimes, as shown in Fig. 16.17: I creep rate decreasing with time (primary creep); II creep rate nearly constant (secondary creep); III increasing creep rate leading to fracture (tertiary creep). Creep increases under increasing load (Fig. 16.18(a)), and increasing temperature (Fig. 16.18(b)). Two other ways of showing creep data are given in Fig. 16.19. Plotting creep compliance (strain/stress) in Fig. 16.19(a) shows the extensibility increasing with time, stress and temperature. A Sherby-Dorn graph, introduced by Wilding and Ward [15, 16], is a log–log plot of creep rate against elongation. Figure 16.19(b) shows creep rate falling to a constant value at high elongations. Measurements of creep recovery by Govaert *et al*. [17] indicated that the creep could be divided into reversible and irreversible elongations (Fig. 16.20). Linearity of the log–log plot shows that each from can be represented by a power law, $\varepsilon(t) \propto t^n$.

Jacobs [13] gives additional information on the effects of molecular weight and draw-ratio on creep of HMPE fibres. Increasing either will reduce creep, but makes fibre production processes more difficult. Creep can be reduced by using branched polyethylene or by crosslinking, but both have other disadvantages.

16.3 Stress relaxation

When a fibre is held stretched, its stress gradually decays. It may drop to a limiting value or may disappear completely. This phenomenon is known as relaxation.

Meredith [18] described an experimental procedure for investigating this. Attached to one end of the specimen, which was usually 20 cm long, was a strong spring. On the release of a catch, the spring extended the specimen to a stop fixed at a known

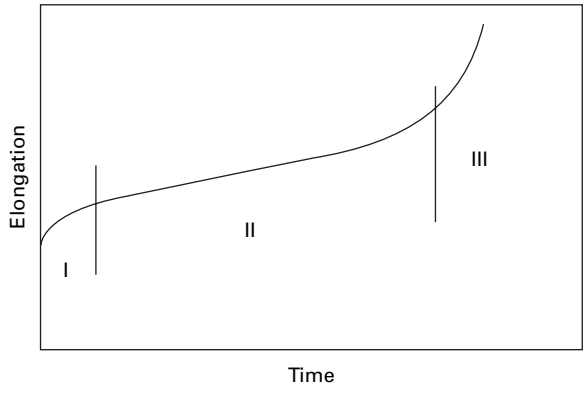

16.17 Three regimes in creep of HMPE fibre [13].

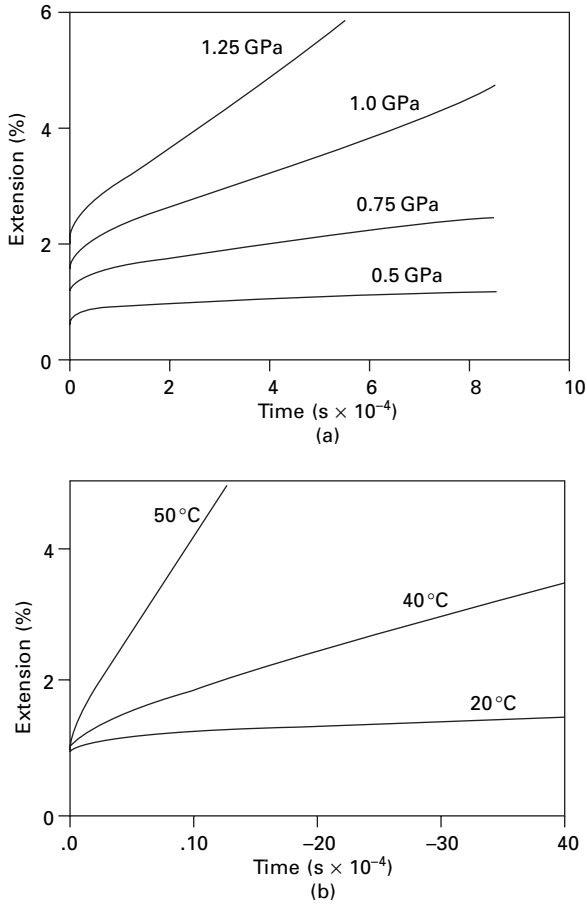

16.18 (a) Creep of *Dyneema* SK66 at 30 °C under various loads. (b) Creep of *Dyneema* SK75 under 0.6 GPa at various temperatures [12].

extension. The extension of the specimen took less than 10 milliseconds, and thus the relaxation of the stress, indicated by a cantilever and mirror system, could be recorded from very short times up to a day.

Figure 16.21 shows a typical result for stress plotted against time. From this it appears that, after a rapid initial decay of stress, the rate of decay drops to zero. In fact, on plotting on a logarithmic scale, as in Fig. 16.22, it becomes clear that the stress is still decreasing after 24 hours. Meredith stated that the stress had not reached a constant value after 2 weeks. It will be seen that, between 1/10 and 10^5 s, the decrease in stress is of the order of 50%, the exact percentage varying with the fibre and the extension.

The curious behaviour of acetate yarn, in which the stress in the first part of the test decays more rapidly at the higher extensions, so that after 1 s the stress is greater for a 2% extension than it is for larger extensions, is believed to be due to a temperature effect. A rapid extension beyond the yield point, with a large energy loss, causes a

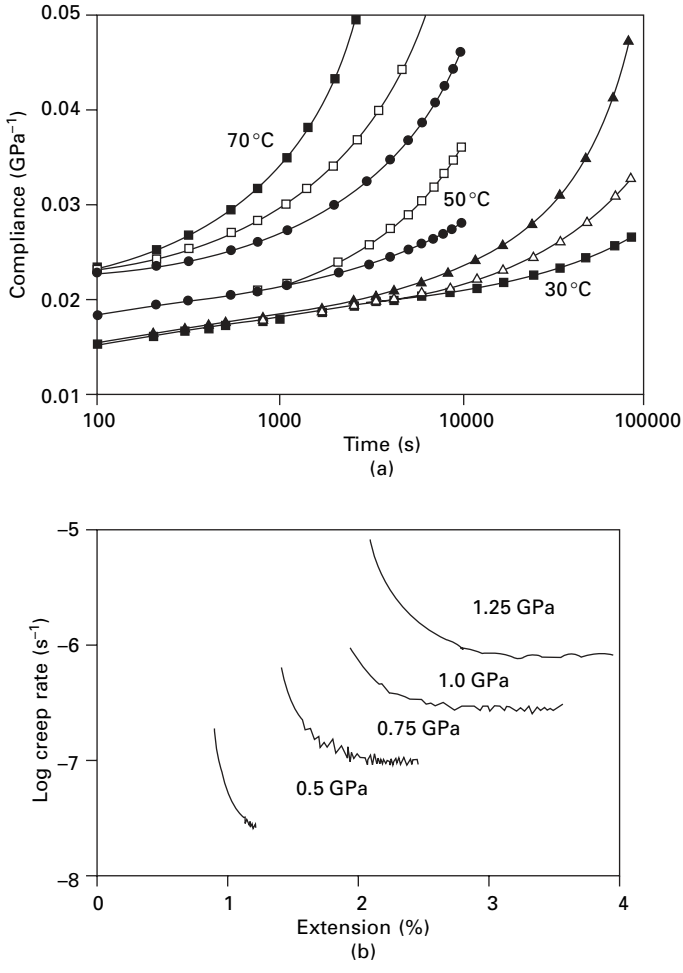

16.19 (a) Creep compliance of *Dyneema* SK66 at different temperatures and stresses. • 0.25 GPa; □ 0.4 GPa; ■ 0.5 GPa; △ 0.75 GPa; ▲ 1 GPa. From Jacobs [13] replotted from [14]. (b) Sherby-Dorn plot for creep of *Dyneema* SK66 in Figure 16.18 (a). From Jacobs [13] replotted from [14].

rise in temperature of the order of 11 °C for a 20% extension. It takes several seconds for the excess heat to be lost from the specimen, so that the initial part of the relaxation curve could be considerably affected.

Figure 16.23 illustrates the relaxation of wool fibres in water at various temperatures by plotting the ratio of the stress at a given time to the stress after 1 h against time on a logarithmic scale. There is considerable scatter in the results obtained on different fibres. The rate of relaxation increases as the temperature increases.

Feughelman [20] has pointed out that the effective initial modulus lies between high and low values, depending on the amount of time allowed for relaxation. The limiting values are the same for all humidities, but the relaxation time is about 500 min at 0% r.h., 100 min at 65% r.h 40 min at 90 r.h., and less than 1 min at 100% r.h.

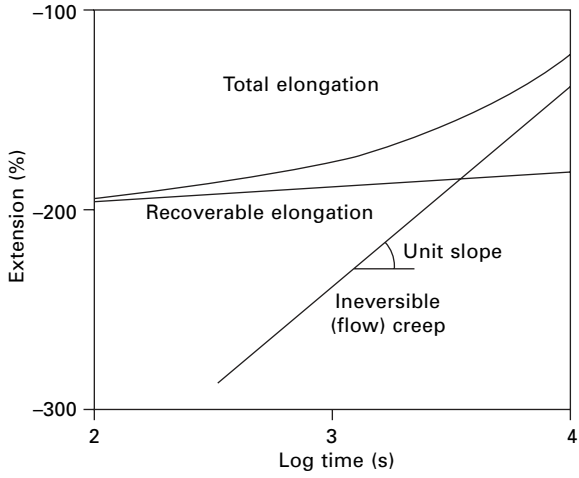

16.20 Recoverable and non-recoverable creep of HMPE fibres. From Jacobs [13].

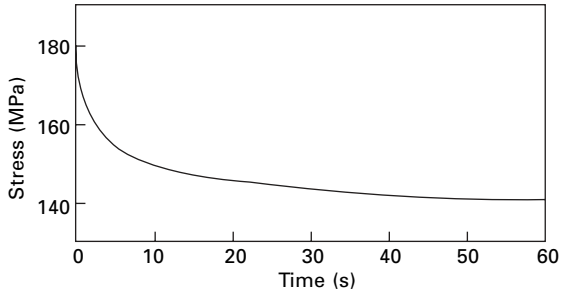

16.21 Stress relaxation in viscose rayon [18].

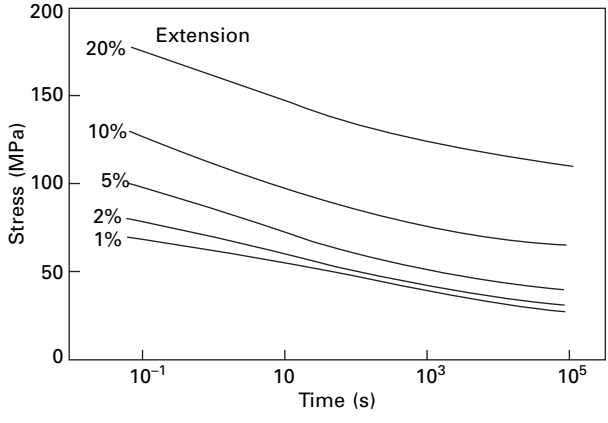

16.22 Stress relaxation in viscose rayon plotted against time on a logarithmic scale [18].

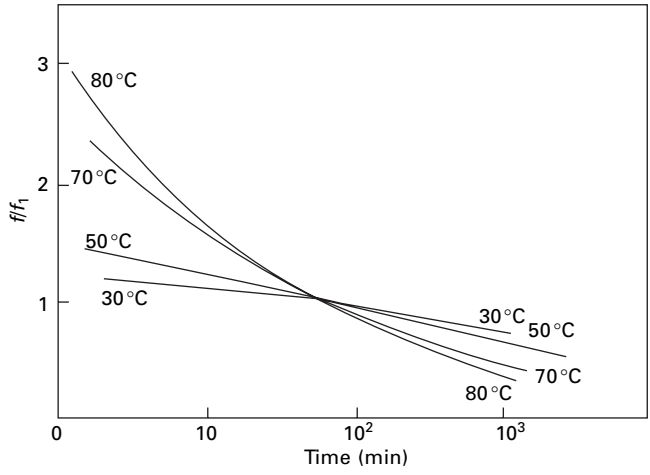

16.23 Relaxation of wool fibres in water with 15% extension at various temperatures [11] (f/f_1 is the ratio of the stress after the given time to the stress after 1 h).

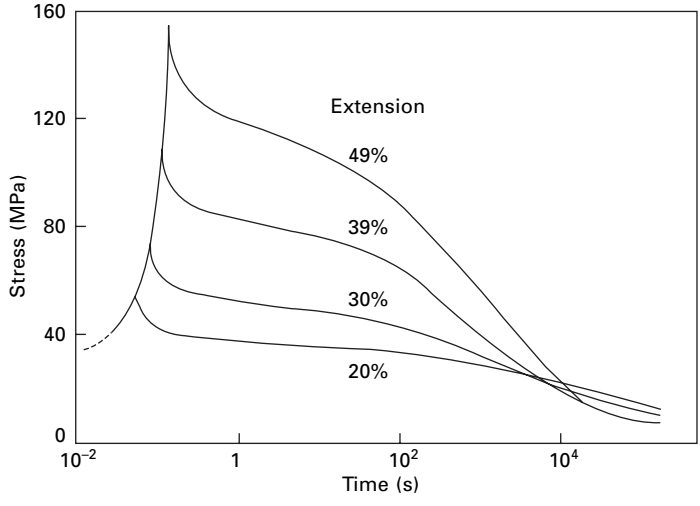

16.24 Relaxation of human hair in water at 35 °C [21].

Figure 16.24 is an example of the relaxation behaviour of human hair in water, as studied by Wood [21]. It will be seen that the curves have a rather complicated shape, with two points of inflection –one between 1 and 10 s, and one between 1000 and 10 000 s.

The stress relaxation of nylon and polyester fibres at a range of temperatures and humidities has been studied by Meredith and Hsu [22]. The data for the polyester fibre relaxing at different strain levels may be presented as a composite sigmoidal curve as shown in Fig. 16.25. The curve as drawn is correct for relaxation at 1% extension, but for other extension values it must be shifted along the time-axis by an

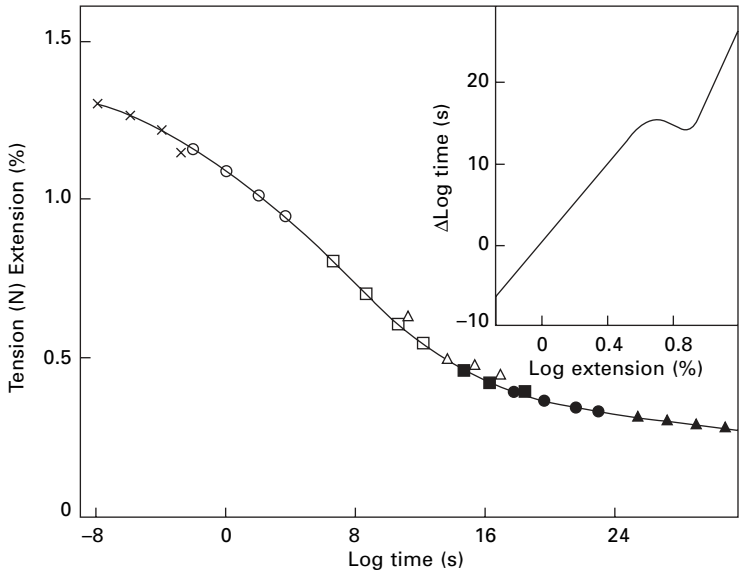

16.25 Composite stress–relaxation curve for a mechanically conditioned 150 den (17 tex) Terylene polyester fibre yarn at 65% r.h. and 25 °C. The separate points are for tests for relaxation from different extensions. From Meredith and Hsu [22].

amount ($\Delta \log t$) shown in the inset graph. Superposition was not possible in this way for the nylon data, but Murayama *et al.* [23] were able to superpose stress relaxation curves for nylon for a constant extension of 2% at different temperatures. Both Murayama *et al.* [24] and Pinnock and Ward [25] have used time–temperature superposition on polyester fibre data. Figure 16.26 shows stress relaxation of nylon 6 [26]. A fast rate of elongation was used, so that measurement started at 0.1 seconds and continued for 1 day. The percentage decrease in stress is almost constant from different starting stresses and is almost the same for stress relaxation in water.

Figure 16.27 shows stress relaxation on polyester (PET) and nylon 6 fibres reported by van Miltenburg [27]. At various imposed elongations, stresses were monitored at 1 second intervals over 100 minutes and are shown as percentages of the stress at the start of the relaxation. In both fibres, the rate of stress relaxation increases rapidly to a maximum value (minimum in the residual stress plot) at around 2% extension. The changes correlate with values of the tangent moduli shown in the lower plots. A similar correlation was found for viscose rayon. Plots of the stress relaxation of HMPE and aramid fibres are shown in Figure 16.28. There was no correlation with tangent modulus, but these fibres have a different structure so that different mechanisms can be expected.

As described in Section 13.5.6 and shown in Fig. 13.29 and others, the stress–strain curves of nylon and polyester fibres may or may not show a minimum in the tangent modulus, depending on the prior treatment of the fibre. The nylon 6 fibre in Figure 16.26 has an almost constant tangent modulus, which would correlate with the lack of change of stress relaxation with starting stress.

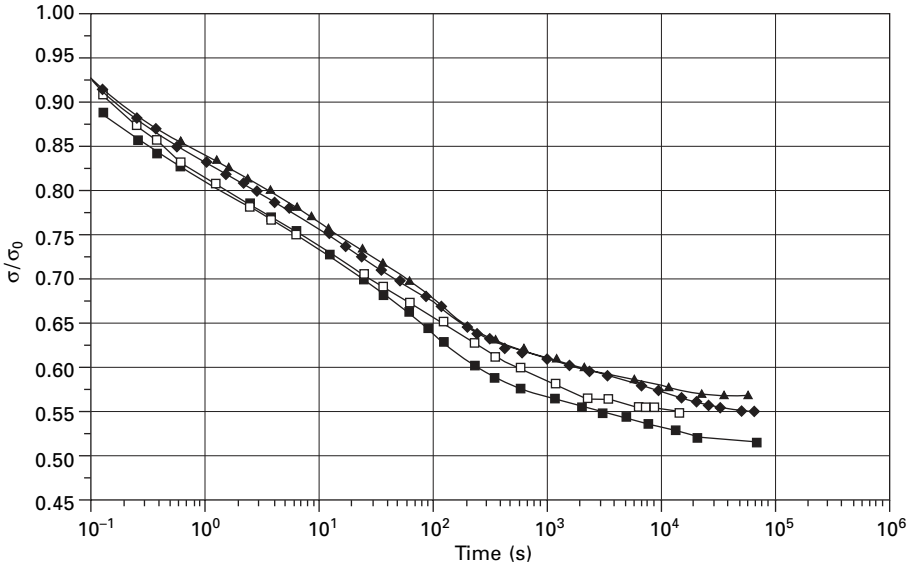

16.26 Stress relaxation of nylon 6 in air at 65% r.h., 20 °C. From 0.96 cN/dtex □; 2.25 cN/dtex ▲; 2.99 cN/dtex ◆; 4.13 cN/dtex. After Selden and Dartman [26].

As demonstrated in Fig. 16.29, when a fibre is extended (OA) and immediately retracted (A→B→…..→G→H→I) at the same rate, it may show *inverse relaxation*. When retraction is stopped between A to P, the stress decreases as usual in stress relaxation. From P to Q, the stress first increases and then decreases. Beyond Q, there is only inverse relaxation. In the final section from G back to the original length at I, the fibre will buckle under zero tension. Nachane and Sundaram [28, 29] report on relaxation and inverse relaxation in polyester fibres and represent the behaviour by empirical equations with exponential terms. Whereas in extension the molecular structure is pulled into a less favourable state, from which it can relax towards equilibrium at a lower stress state, in substantial retraction it goes back beyond the equilibrium state and so the stress increases in inverse relaxation. The actual molecular mechanisms may be quite complicated.

16.4 Time and tensile testing

16.4.1 High-speed tests

At low speeds, that is, for tests lasting more than a few seconds, the conventional methods described in Chapter 13 can be used. At higher speeds, other methods must be adopted.

One way is to use an impact test. In this method, a moving large mass is engaged with one end of the specimen, while the other end is held fixed and connected to a load-measuring device. There must be appropriate mechanical arrangements to ensure that the free jaw is engaged only after the mass has attained its required speed. The moving mass may be a rotating flywheel [30], the bob of a pendulum [31], a falling

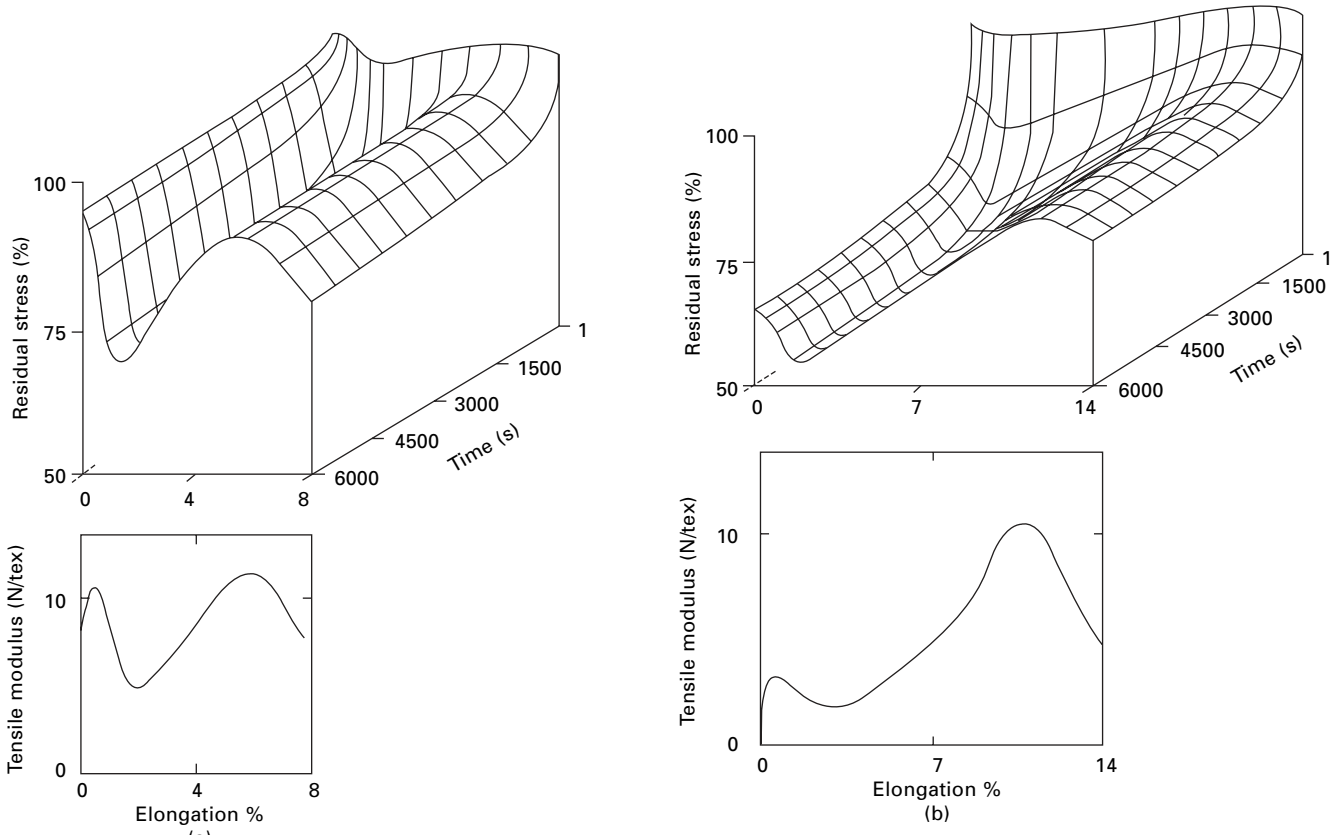

16.27 Upper diagrams: stress relaxation plotted against elongation and time to 100 minutes. Lower diagrams: tangent modulus plotted against elongation: (a) polyester (PET) yarn; (b) nylon 6 yarn. From van Miltenburg [27].

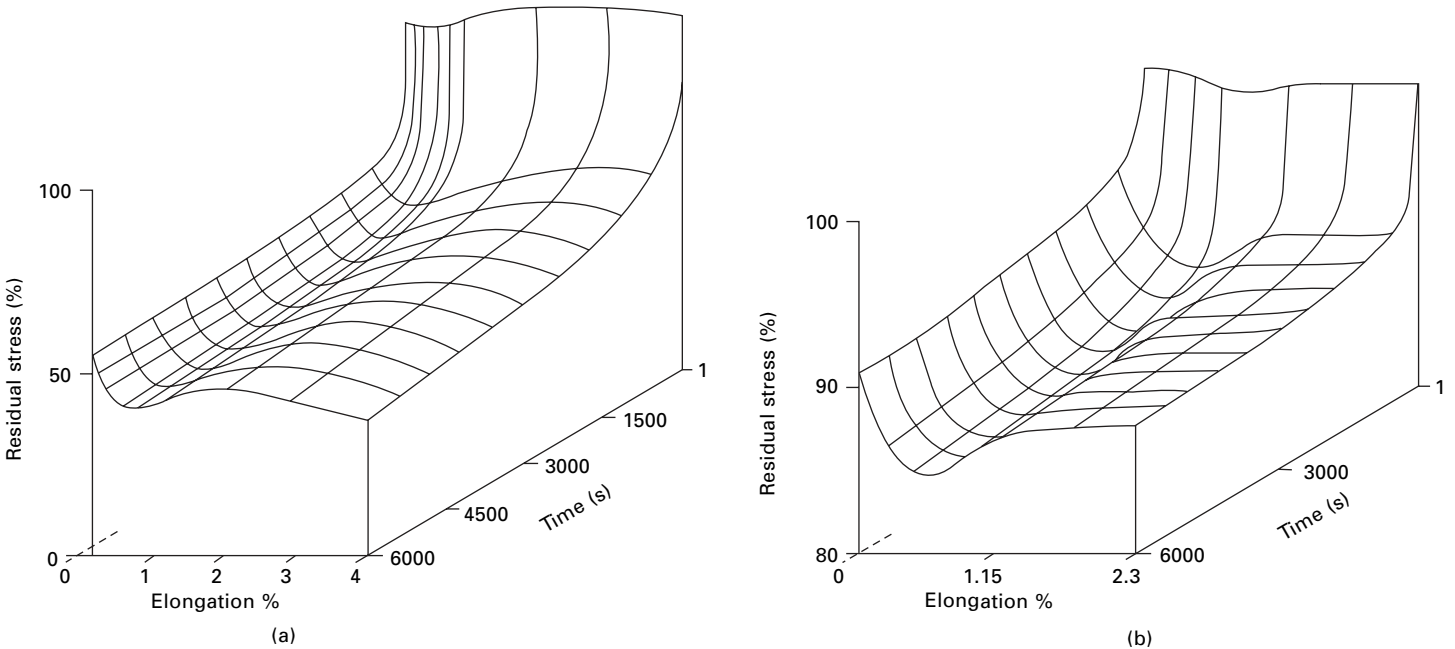

16.28 Stress relaxation plots over 100 minutes for: (a) gel-spun HMPE fibre; (b) aramid fibre. Note the scale difference: HMPE drops to a low of 40%, but aramid only to 85%. From van Miltenburg [27].

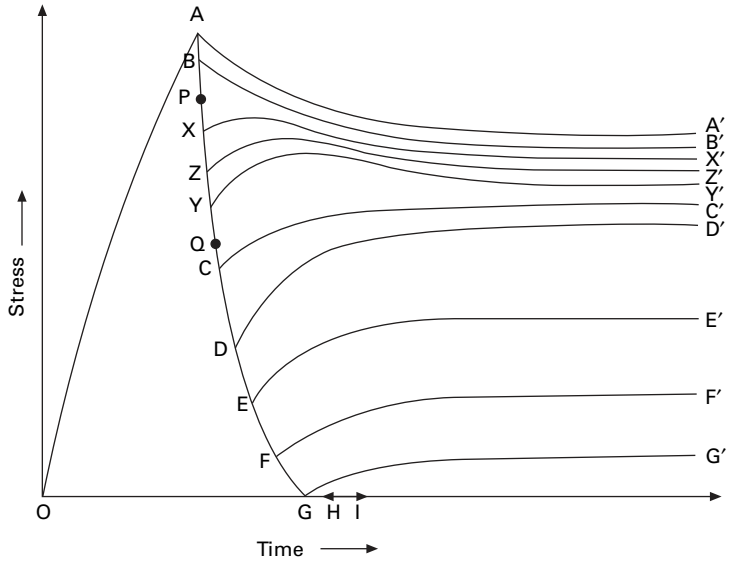

16.29 Inverse relaxation of polyester. From Nachane and Sundaram [28].

weight [32] or a rifle bullet [33–36]. In the past, the load measurement could be by means of a cantilever arm and mirror, recording on photographic paper, or by a resistance strain-gauge, a capacitive or inductive pick-up, or a piezo-electric crystal, connected through an appropriate circuit to an oscilloscope. Nowadays, digital recording would be used. If the weight is massive, its speed will not change on breaking the specimen, and thus there will be a constant rate of extension. If the recorder or oscilloscope has a linear time-base, it will record the load–elongation curve directly. In this way, rates of extension of from 10 to 3000% per second can be obtained.

At still higher rates of straining, the velocity of transmission of the strain along the specimen becomes important, and more complicated experimental arrangements are necessary. Schiefer and his colleagues [37–40] have been able to work out stress–strain curves at rates of straining of 1000–15 000% per second from successive photographs of the configurations of a clamped length of yarn subjected to a transverse impact. They had made earlier investigations at similar rates of straining by determining the lowest velocity of impact at which a yarn would break when one end was impacted, the other end being either free or attached to a small free mass.

Mi [41] adapted a catapult method, originally developed by Stevens and coworkers [42, 43] for heavy duty testing, for a study of wave propagation in twisted yarns. The essential principles of the method, which could be used to determine stress–strain relations, are shown in Fig. 16.30. A driving member (*Kevlar* cord), which is highly stretched, is joined to the test specimen by a clamped connector. When the clamp is released, the driving member rapidly contracts, thus extending the test specimen at a high rate. Force and displacement are recorded. The elongation velocity can be varied by altering the pre-strain of the driving member, but is limited by the mass of the connector. The deformation of the much lighter test specimen has little effect on the rate. The typical time for the connector to reach the stop was 1 millisecond. The

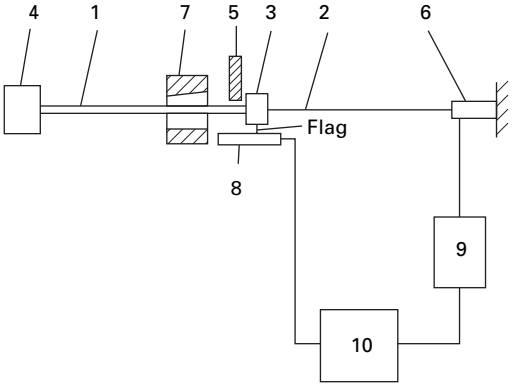

16.30 Catapult test method. 1, driving member; 2, test specimen; 3, connector; 4, stretching device; 5, quick release clamp; 6, force transducer; 7, stop device; 8, displacement detector (optical switches); 9, charge amplifier; 10, oscilloscope. From Mi [41].

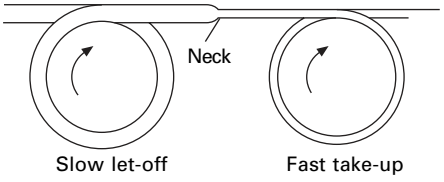

16.31 Drawing of synthetic fibre.

initial rise in force and elongation is followed by a damped oscillation due to the impact of the clamp on the stop. If the stop was not present, elongation could proceed to break, but safety precautions would be needed.

16.4.2 Temperature and time: isothermal and adiabatic changes

In an imperfectly elastic material, energy will be dissipated in internal friction when the material is extended. This energy is represented by the area inside a hysteresis loop and is turned into heat. In a slow test, this heat will be given off to the surroundings and there will be no appreciable change of temperature of the specimen, but in a rapid test there will be less opportunity for loss of heat and the specimen will rise in temperature. Experiments thus range between two limiting cases: the isothermal, with no change of temperature, and the adiabatic, with no loss of heat. Since the properties of a fibre vary with temperature, the results obtained in the two types of test will be different, and this must be remembered in interpreting the effect of time.

An interesting example of adiabatic (or nearly adiabatic) conditions occurs in the drawing of fibres. Marshall and Thompson [44] have shown that it offers an explanation of the occurrence of characteristic draw-ratios. The process is illustrated in Fig. 16.31. Any attempt to alter the draw-ratio by changing the relative speeds of the rollers merely results in the neck's moving backwards or forwards, the actual draw-ratio remaining constant. If the neck reaches the back roller, the filament breaks, and,

if it reaches the front roller, intermittent portions of undrawn material pass through. In either case, the technical consequences are serious.

Figure 16.32 shows the isothermal stress–strain curves for (undrawn) polyester fibre. If extension takes place adiabatically, however, the temperature rises and the path OABC should be followed. But, under actual drawing conditions, a decreasing load is an unstable condition, so that the line AC is followed. It is this sudden increase in length past the unstable region ABC that results in the formation of a neck and determines the characteristic draw-ratio. If the whole process is slowed down, there will be some loss of heat, the temperature rise will be smaller, and thus the draw-ratio will be reduced. This is found in practice. The draw-ratio is also affected by the mean temperature at which the drawing is carried out.

Godfrey [45] examined the effect of heat dissipation during plastic deformation, taking account of heat transfer to the surroundings. The model assumes that the fibre behaves in the idealised elastic/plastic way shown in Fig. 16.33, with the plastic stress line decreasing linearly with increase of temperature. Figure 16.34(a) shows that, for a 7.2 dtex nylon fibre, the deformation is close to isothermal at a rate of extension of 10% per second and close to adiabatic at 500% per second. Figure 16.34(b) shows the reduction in tension as the specimen heats up. Godfrey's numerical data is expressed in terms of a dimensionless temperature rise, $\Delta T/T$, and a dimensionless time, t^*, which is proportional to imposed strain and depends on fibre dimensions, thermal and mechanical properties, and ambient conditions. For a thick (195 tex) nylon yarn, there is appreciable heating at a strain rate of 10% per second.

There may also be a difference, analogous to the difference between adiabatic and isothermal changes, due to the influence of moisture. As was discussed in Section 12.3.2, the equilibrium regain of a fibre at a given vapour pressure depends on the stress in the fibre. On the application of a tension to a fibre, its equilibrium regain increases. Consequently, there will be a difference between tests made rapidly, which

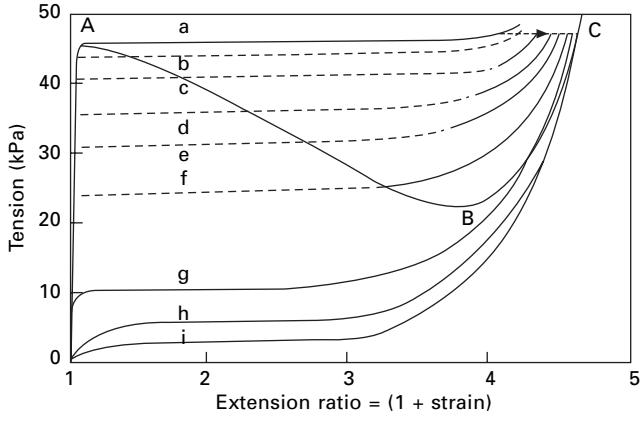

16.32 Isothermal and adiabatic load–extension curves of *Terylene* polyester fibre. Isothermals: a, 20 °C; b, 30 °C; c, 40 °C; d, 50 °C; e, 60 °C; f, 70 °C; g, 80 °C; h, 100 °C; i, 140 °C. Adiabatic: (A) from 20 °C. (Dotted portions obtained by interpolation).

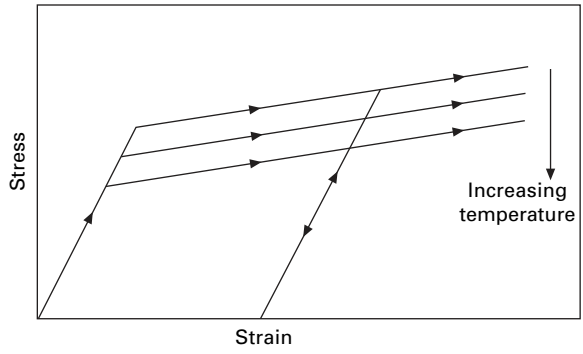

16.33 Idealised fibre stress–strain curve with yield stress decreasing linearly with temperature.

will be at constant regain, and those made slowly, which will be at constant vapour pressure. Since the change in regain with tension is very small, the difference between the two will be small in tensile tests. A loss of moisture due to adiabatic heating would have a larger effect.

16.4.3 Influence of rate of loading on breakage

The breaking load of a fibre depends on the rate at which the load is applied. As a first approximation, we can say that the breaking extension is independent of the rate of loading. If we apply a constant load to a fibre, we get the behaviour shown in Fig. 16.35, that is, instantaneous extension followed by creep and then, when the critical extension is reached, breakage. The time for this to happen will be shorter the greater the load. Thus the time to break decreases with increasing load.

There is a similar effect in testing when the load is increased throughout the test. If the rate of increase of load is slow, there is more time for creep to occur, and consequently the breaking extension is reached at a lower load. The breaking load therefore increases as the rate of loading increases.

Meredith [30] tested yarns over a millionfold range of rates of extension and found that the relation between tenacity and rate of extension was approximately linear (actually slightly concave to the tenacity axis) for most fibres. For breaking times ranging between a second and an hour, the following formula may be used without much error:

$$F_1 - F_2 = kF_1 \log_{10}(t_2/t_1) \tag{16.5}$$

where F_1 is breaking load in a time t_1, F_2 is breaking load in a time t_2, and k is the *strength–time coefficient*.

Values of the strength–time coefficient are given in Table 16.3. They show that the strength of these textile fibres increases by 6–9% for each tenfold increase of rate of extension. Meredith stated that the same formula applies to constant rate of loading and constant rate of extension tests.

Some values of tenacity and other tensile properties obtained in Schiefer's very

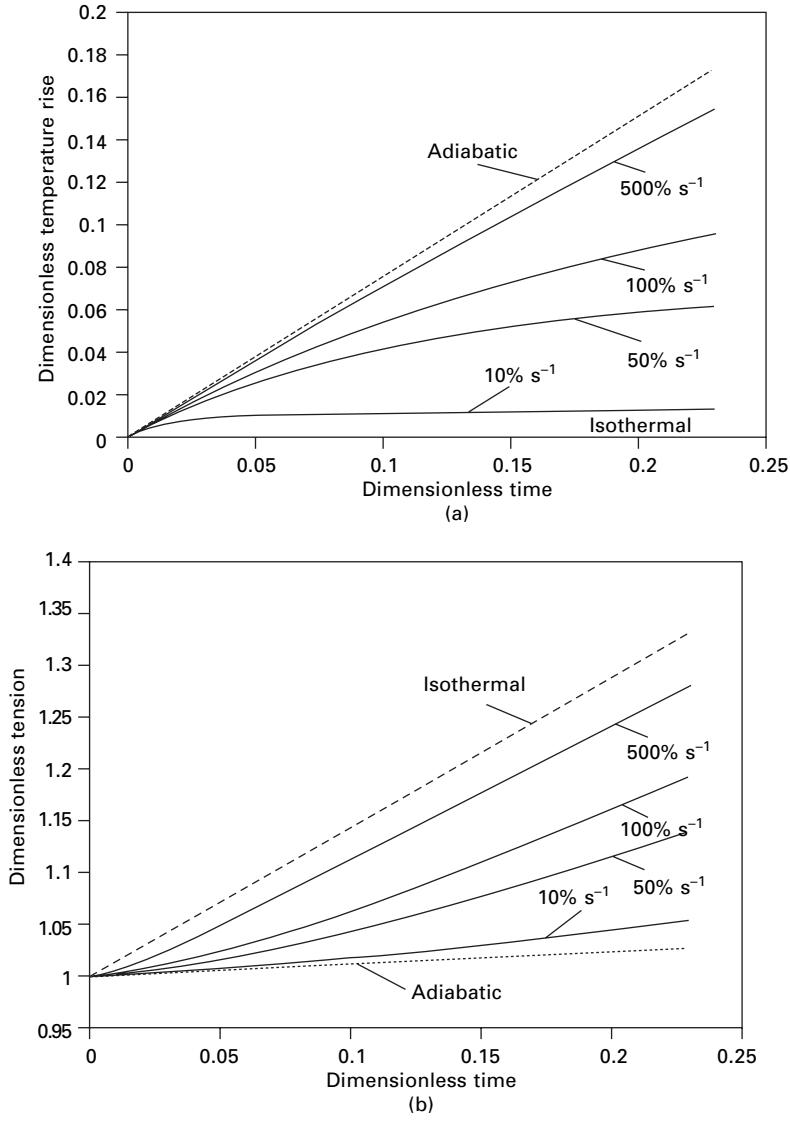

16.34 Simulated response of 7.2 dtex nylon fibre extended at various strain rates. Adapted from Godfrey [45].

high-speed tests are given in Table 16.4, together with comparative values obtained in ordinary tests. The increase in strength and modulus means that performance in ballistic testing is better than expected from low-speed tests, though the reduction in breaking extension will act in the opposite way. The counterpart to this is that performance will be worse for long-term loading as in mooring oil-rigs. Table 16.5 shows expected time to break under various percentages of the 1 minute break load. It is estimated that k is less than 0.05 for aramid yarns and slightly more for polyester. Since safety factors are below 50%, creep rupture is not significant for this application.

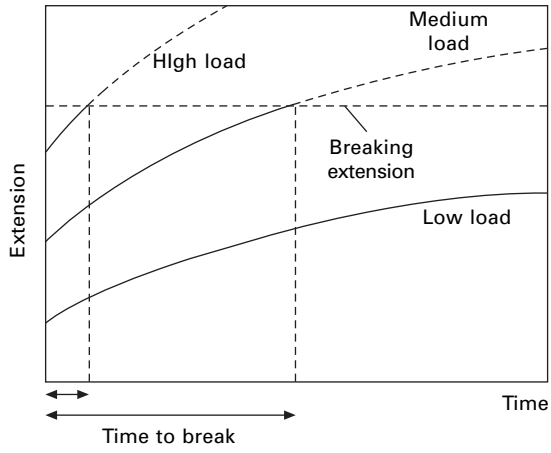

16.35 Breakage of fibre under various loads.

Table 16.3 Strength–time coefficients [46]

Material	*k*
Cotton	0.088
Viscose rayon	0.083
Acetate	0.060
Flax	0.079
Silk	0.079
Nylon	0.080
Wool	0.073

Table 16.4 Results of high-speed tests [32]

Material	Rate of straining (% per second)	Tenacity (N/tex)	Breaking extension (%)	Initial modulus (N/tex)
High-tenacity nylon	1/60	0.55	16.7	3
	5000	0.67	14.7	5
Fortisan (highly oriented)	1/60	0.56	5.4	14
cellulose)	2000	0.80	5.2	22
Fiberglas	1/60	0.42	2.8	22
	1000	0.54	1.8	28

Table 16.5 Creep rupture. From TTI and Noble Denton [11]

	Time to fail at percentage of 1 minute break load			
k	20%	30%	50%	80%
0.05	2×10^{10} years	2×10^{8} years	2×10^{5} years	200 hours
0.08	2×10^{4} years	1000 years	3 years	5 hours
0.1	200 years	19 years	60 days	100 minutes

In a fatigue test, when some fibres in an assembly have broken, the increased stress on the remaining fibres leads to creep rupture as the final failure mechanism. For nylon, the loss of strength is marginal.

HMPE fibres do not follow equation (16.5), but fail more rapidly than a value of $k = 0.1$ would indicate. Creep rupture in long-term loading is a serious concern. Figure 16.36 shows how the strength of HMPE fibres at 21 °C has a tenfold decrease in strength between normal testing speeds and a rate of strain of 10^{-7}% per second, which corresponds to a time to break of about 1 year. Figure 16.36 also shows the large influence of temperature. At lower temperatures in the sea, break would take longer, but in warm conditions it would occur sooner. Schwartz *et al*. [48] found that the strength of *Spectra* 900 increased from 2.13 GPa at a strain rate of 0.4% per minute to 3.34 GPa at 100% per minute. They express the results by a Weibull distributions associated with a power law breakdown rule.

The rate of extension affects the breaking extension in different ways for different fibres. Thus, in an acetate yarn, the breaking extension, which was about 30%, varied by less than 0.5% for rates of extension between 0001 and 1000% per second, but in a viscose rayon yarn the breaking extension increased from 20.6 to 26.6%, and in a silk yarn it increased from 15.3 to 23.1%, over the same range. In a nylon yarn, the breaking extension increased from 15.9% at 0.0013% per second to 20.7% at 22% per second and then decreased to 14.5% at 1096% per second. Where the strength increases with the rate of extension and the breaking extension is constant or increases, then the work of rupture will be greater in the more rapid breaks, but, in nylon at high speeds, the decrease in the breaking extension has a greater effect than the increase in breaking load, and the work of rupture decreases. This must be considered where fibres are used under impact conditions.

16.4.4 Stress–strain curves

Stress–strain tests take some time, and consequently there is an opportunity for creep to occur. The slower the test, the more time there is available, and thus the greater the

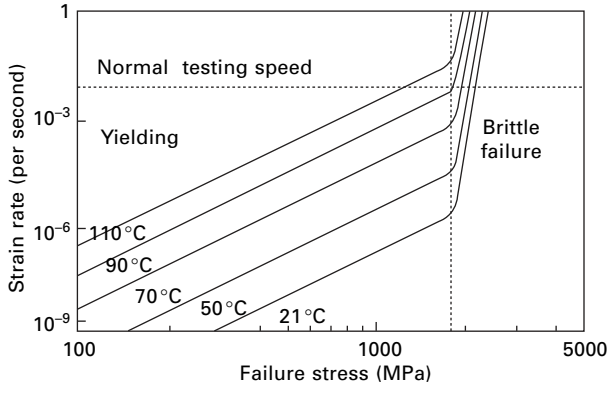

16.36 Effect of strain rate and temperature on breakage of HMPE (Dyneema) yarn. From van Dingenen [47].

extension at a given load. This is illustrated in Fig. 16.37, which shows results for viscose rayon, acetate, silk and nylon. Because of creep, the slower curves are nearer to the strain axis than the faster curves. This effect is particularly marked at the higher loads. There are two reasons for this. Near the end of the test, there has been more time for creep, and above the yield point the rate of creep is greater.

If the stress–strain curves are non-linear, there will also be a difference between constant rate of loading and constant rate of extension tests, owing to the different proportions of time spent on different parts of the curves. For a stress–strain curve that bends towards the strain axis, as in Fig. 16.38(a), we see that a greater proportion of the time is spent on the part of the curve at high loads in a constant rate of extension test than is the case in a constant rate of loading test. In the example shown, three-quarters of the time is spent above the point A and one-quarter below it, compared

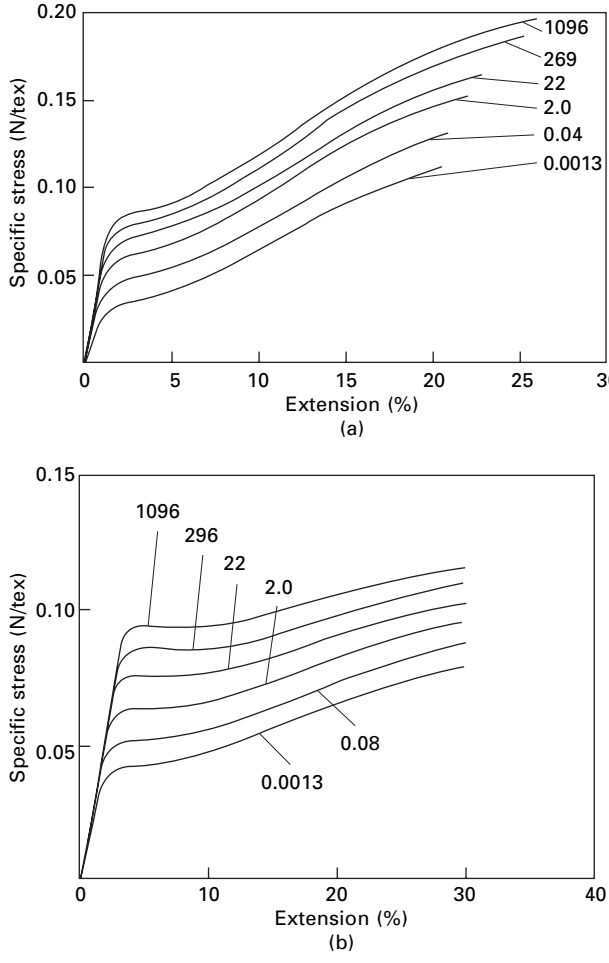

16.37 Stress–strain curves at various rates of extension [30]: (a) viscose rayon; (b) acetate; (c) silk; (d) nylon. The figures against the curves refer to the percentage rates of extension per second.

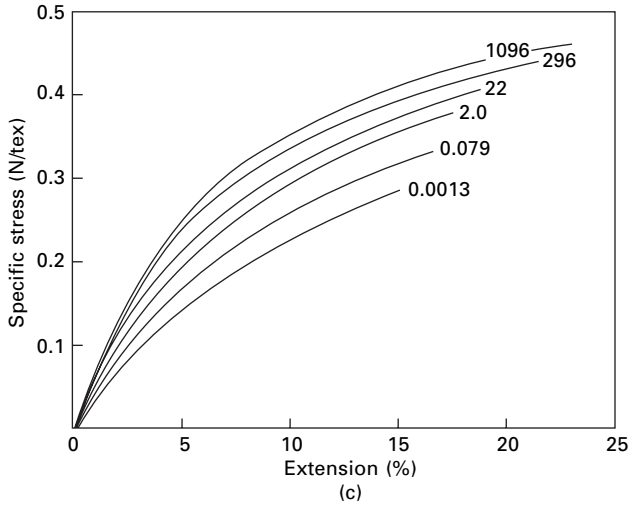

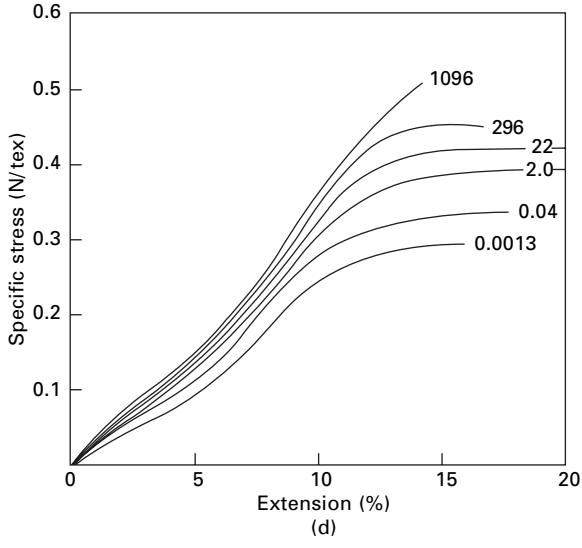

16.37 (Continued)

with the reverse proportions in a constant rate of loading test. The result of this is that, in a constant rate of extension test, whereas there will be slightly less creep in the early stages, there will be a greater total amount of creep at the end of the test, since the rate of creep is greater at high loads. The two curves will therefore differ as shown in Fig. 16.38(b).

The stress–strain curves obtained for a fibre thus depend on the time taken in the test and on the way in which the time is distributed. There will be consequent effects on the quantities, such as modulus and yield point, derived from the curve. An example of the change in Young's modulus (up to 1% extension) of wet wool with rate of extension is shown in Fig. 16.39. Meredith [30] also found that the initial

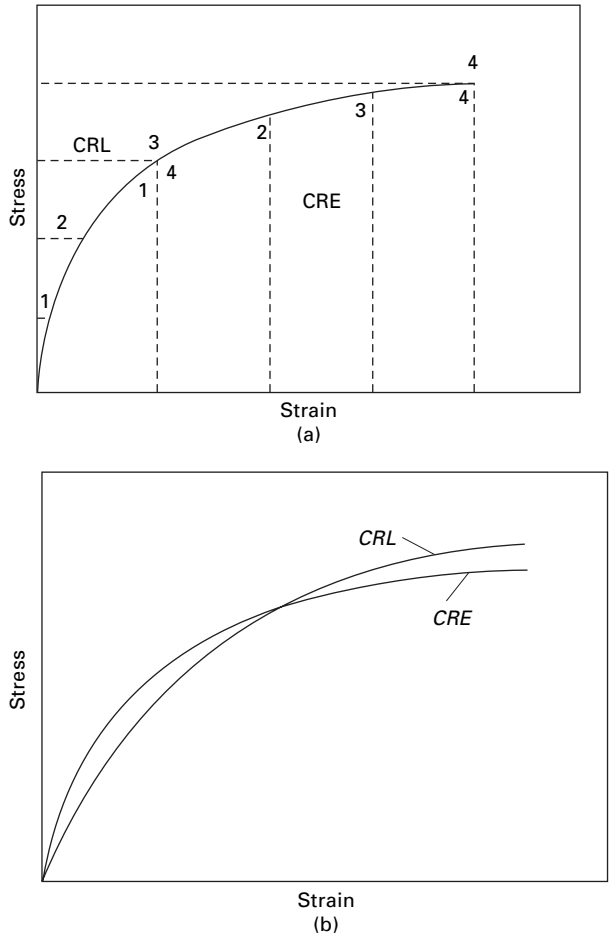

16.38 (a) Stress–strain curve showing equal intervals of time at constant rate of loading (CRL) and constant rate of elongation (CRE). (b) Difference between CRL and CRE curves.

modulus increased almost linearly with log (rate of extension). Values of the initial modulus obtained by Schiefer *et al.* [32] are included in Table 16.4. In viscose rayon and acetate, the yield points occur at increasingly higher stresses as the rate of extension increases, but the parts of the curves beyond the yield point are almost parallel.

Hall [35] found that it was possible to express the stress–strain curves of rayon, nylon, polyester, acrylic and polypropylene fibres, at 12 rates of strain between 10^{-2} and 50 000% per second, by equations of the form:

$$\frac{\sigma}{\varepsilon} = \frac{f_2(\varepsilon) + f(t)}{f_1(\varepsilon)} \tag{16.6}$$

where σ, ε and t are stress, strain and time, respectively. Hall's experimental results [50] for polyester and acrylic fibres are shown in Fig. 16.40.

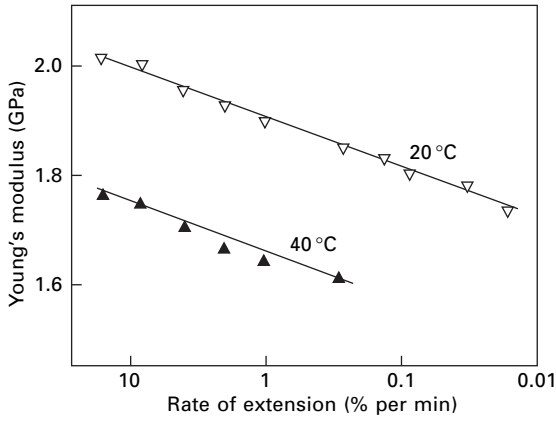

16.39 Change of modulus of wet wool with rate of extension [49]: note that *x*-axis is for decreasing rate.

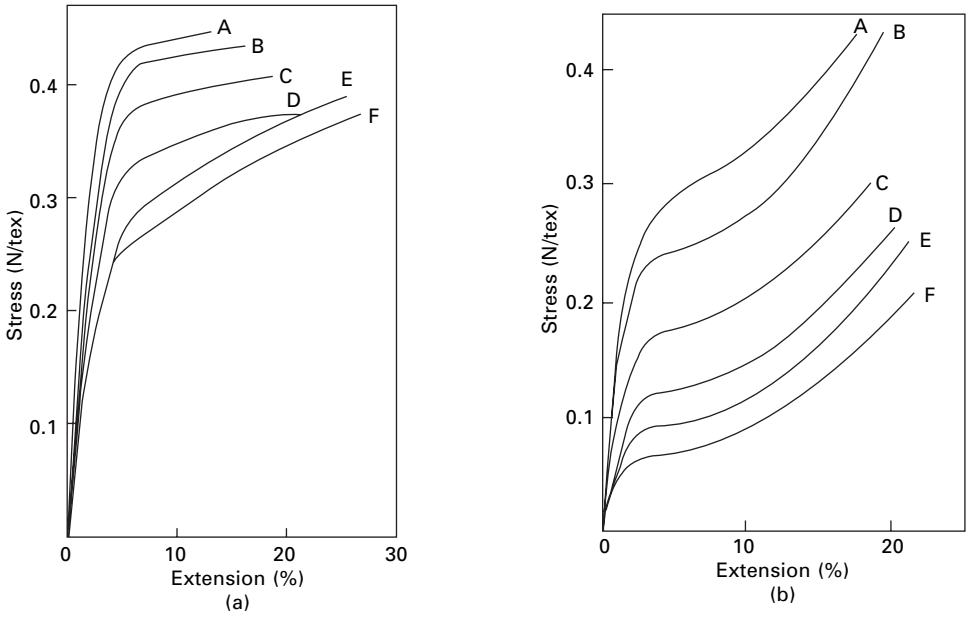

16.40 Stress–strain curves at various rates [50]: (a) polyester fibre: A, 23 000; B, 6400; C, 120; D, 7.7; E, 1.3; F, 0.018 % per second; (b) acrylic fibre: A, 60 000; B, 7500; C, 420; D, 7.7; E, 0.99; F, 0.001 % per second.

Determinations of stress–strain curves at high rates have also been reported by Holden [36], Smith *et al.* [34, 51] and Skelton *et al.* [52]. Smith *et al.* [51] found that, at a rate of extension of 4100% per second, polyester fibre yarn broke at 8% extension, without any yield region and at a higher strength level than in the fracture at low speed with breakage at 20% extension. The change in mode of fracture of nylon and polyester fibres is described in Section 19.2.1.

16.5 Dynamic tests

16.5.1 Static and dynamic testing

In the conventional methods of testing described in Section 13.4 and most of the high-speed tests described in Section 16.4.1, although the time of application has influenced the result, it has been possible to observe directly the stress–strain relation without considering the equation of motion of the system. Consequently, these tests may be described as static (or quasi-static) tests. There are, however, other tests in which the equation of motion must be considered, and these are one type of dynamic test. However, if there is a monotonic increase of stress, they are considered with the static tests. The high-speed impact tests described in Section 16.4.5 are examples of this situation. It is necessary to take account of the dynamic effects when the inertia, either of part of the apparatus or of the specimen, cannot be neglected. Thus the inertia effects involved in old-fashioned pendulum testers or in inclined-plane testers (Section 13.4.3) are examples of the occurrence of dynamic effects as sources of error in what are intended to be static tests. The dynamic tests dealt with in this section are of two types: (1) cyclic loading and (2) tests in such a short time that the propagation of the stress wave means that the stress cannot be regarded as constant along the specimen.

16.5.2 Characterisation of viscoelastic behaviour

It is now necessary to consider how the results of dynamic tests may be expressed. Let stress = f and strain = e at time t. If we apply a sinusoidal extension to the fibre (the converse argument will apply for sinusoidal loading), starting at time $t = 0$, we have:

$$e = e_m \sin \omega t \text{ for } t \geq 0 \tag{16.7}$$

where e_m is the strain amplitude, and ω is the angular frequency in radians/second (equal to $2\pi \times$ frequency in Hz).

In general, the fibre will respond so that the stress f shows (1) an initial transient response; and (2) an ultimate 'steady-state' response, which may have a complex shape and which may change slowly with time owing to the effects of creep and stress relaxation.

The steady-state stress variation will certainly have an amplitude and be related in phase to the imposed extension. In the simplest situation, we can therefore put:

$$f = f_m \sin (\omega t + \delta) \tag{16.8}$$

where f_m is the stress amplitude and δ is the angular phase difference.

Equation (16.8) is only strictly valid for materials that obey the laws of *linear viscoelasticity*. For these materials, the interrelations between the various parameters discussed below will apply correctly, but for non-linear materials, including most fibres except at very small strain, the relations will be only approximately true. It is common practice to interpret the data from dynamic tests as if equation (16.8) were valid, the more complicated functional relation between stress and time being ignored. The differences are indicated in Fig. 16.41.

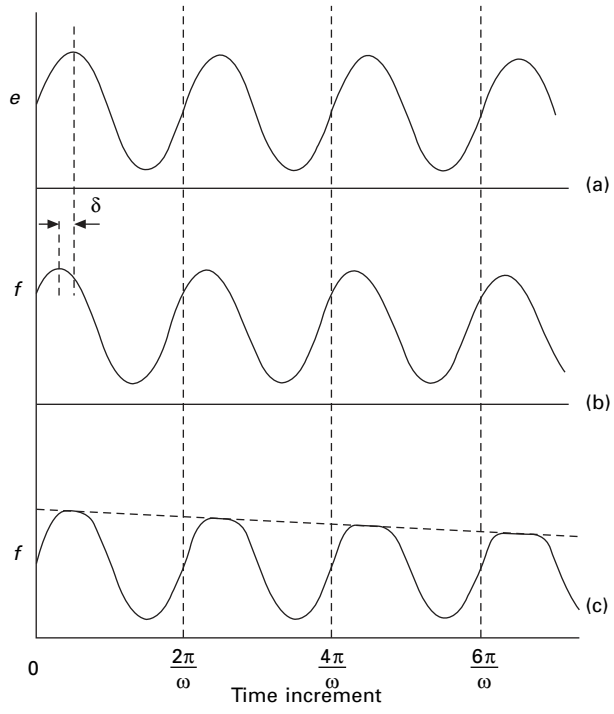

16.41 Dynamic structures and steady-state response: (a) imposed sinusoidal strain variation; (b) stress variation for linear viscoelastic material; (c) stress variation for a non-linear material, showing also a longer-term trend.

Another simplification is to separate the static and dynamic components of the stress and strain. Thus, when a sinusoidal extension is imposed on a constant extension, we have:

$$e = e_0 + e_m \sin \omega t \tag{16.9}$$

$$f = f_0 + f_m \sin (\omega t + \delta) \tag{16.10}$$

In the consideration of dynamic behaviour, the constant parts e_0 and f_0 can be ignored and equations (16.7) and (16.8) used instead of equations (16.9) and (16. 10). This is particularly important in fibres, where the whole nature of the deformation changes owing to buckling if the stress f becomes negative. The dynamic variation must therefore always be superimposed on a static loading.

The subject is complicated by the number of ways in which the dynamic behaviour can be represented. We note that, with the above simplification, the response will be given by two parameters, but there are several possible pairs.

Representation (1):

The most direct method of expressing experimentally observed results is by quoting:

modulus from ratio of amplitudes = f_m/e_m

phase angle or loss angle = δ

However, these quantities are less convenient in other ways.

The phase lag is shown up as a hysteresis loop in the stress–strain relation.

Representation (2)

Equation (16.8) transforms to:

$$f = f_m (\cos \delta \sin \omega t + \sin \delta \cos \omega t) \tag{16.11}$$

Thus the stress response can be regarded as the addition of a component $f_m \cos \delta$, in-phase with the strain, and a component $f_m \sin \delta$, which is 90° out of phase.

This leads to a definition of the two quantities:

'in-phase' modulus (usually termed *dynamic modulus*)

$$= \frac{\text{in-phase stress amplitude}}{\text{strain amplitude}} = \frac{f_m \cos \delta}{e_m} = E \tag{16.12}$$

ratio of out-of-phase stress amplitude to in-phase stress amplitude (usually termed *loss factor* or *dissipation factor*)

$$= \frac{\sin \delta}{\cos \delta} = \tan \delta \tag{16.13}$$

We may note that, in the analogous situation in alternating-current electricity, the quantity usually used is power factor = $\cos \phi = \sin \delta$, where $\phi = (\pi/2) - \delta$.

Representation (3): Voight model

A system that obeys equations (16.7) and (16.8) can be physically represented at any given frequency by an ideal (Hookean) spring, with stress proportional to strain, in parallel with an ideal (Newtonian) dashpot, with stress proportional to rate of strain, as shown in Fig. 16.42. The stress is given additively as:

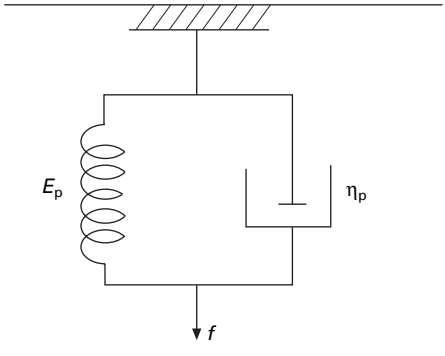

16.42 Parallel combination of spring and dashpot (Voigt model).

$$f = E_p + \eta_p \frac{de}{dt} \tag{16.14}$$

where E_p is the spring modulus and η_p is the viscous coefficient of the dashpot.

Substitution from equation (16.7) gives:

$$f = E_p e_m \sin \omega t + \eta_p \omega e_m \cos \omega t$$

$$= (E_p^2 + \eta_p^2 \omega^2)^{\frac{1}{2}} e_m \left\{ \frac{E_p}{(E_p^2 + \eta_p^2 \omega^2)^{\frac{1}{2}}} \sin \omega t + \frac{\eta_p \omega}{(E_p^2 + \eta_p^2 \omega^2)^{\frac{1}{2}}} \cos \omega t \right\} \tag{16.15}$$

We see that this is the sum of in-phase and out-of-phase components and is similar in form to equation (16.11), which thus proves the equivalence of the representation. The relations between the quantities are:

$$f_m = (E_p^2 + \eta_p^2 \omega^2)^{1/2} e_m \tag{16.16}$$

$$\tan \delta = \frac{\eta_p \omega}{E_p} \tag{16.17}$$

$$E_p = E \tag{16.18}$$

The parameter $\eta_p \omega$ is often used as an alternative to $\tan \delta$ to express the loss properties.

It may be noted that in a creep test, with constant f_0, the basic equation (16.14) of the parallel model has the solution by integration:

$$e = \left(\frac{f_0}{E_p}\right)\left[1 - \exp\left(\frac{-E_p t}{\eta_p}\right)\right] = \left(\frac{f_0}{Ep}\right)\left[1 - \exp\left(\frac{-t}{\tau_p}\right)\right] \tag{16.19}$$

where $\tau_p = \eta_p / E_p$ = creep time constant. There is thus a link between this expression of the dynamic properties and exponential creep behaviour, illustrated in Fig. 16.43.

It must be remembered, however, that this will apply in this simple form if the parallel model is a complete representation of the system at all frequencies. But the

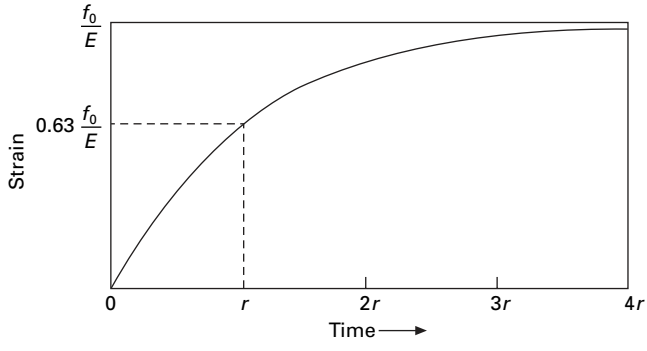

16.43 Behaviour of ideal specimen under constant load.

model was introduced here only to represent behaviour at a particular frequency. In general, the parameters E_p and η will vary with frequency.

Representation (4): Maxwell model

The behaviour at any given frequency can also be represented by an ideal spring in series with an ideal dashpot, as in Fig. 16.44. The basic equation of this model is given by the addition of strains in an infinitesimal increment of time:

$$\frac{de}{dt} = \frac{1}{E_s}\frac{df}{dt} + \frac{f}{\eta_s} \tag{16.20}$$

Substitution of equation (16.7) and rearrangement lead once again to an expression that is similar in form to equation (16.11). The parameters are related by the equations:

$$E_s = E\sec^2\delta \tag{16.21}$$

$$\tan\delta = E_s/\eta_s\omega \tag{16.22}$$

These quantities are less simply related to the other parameters and so are less useful. They do, however, provide a link to stress–relaxation behaviour because, with constant strain τ_0, the solution of equation (16.20) is:

$$f = (E_s e_0)\exp(-E_s t/\eta_s) = (E_s e_0)\exp(-t/\tau_s) \tag{16.23}$$

where $\tau_s = \eta_s/E_s$ = relaxation time constant. But it must again be stressed that, in a real system, the parameters E_s and η_s would vary with frequency, so that the simple relations would not apply.

Representation (5)

In a single cycle, the energy loss per unit volume (or per unit mass, if f is a specific stress and the moduli are in corresponding units) is given, with the notation of equation (16.15), by:

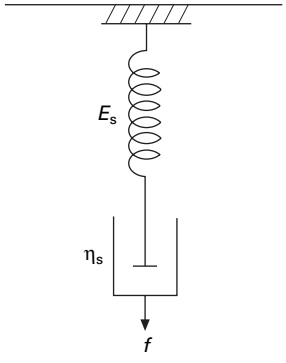

16.44 Series combination of spring and dashpot (Maxwell model).

$$\oint f \, \mathrm{d}e = \int_{t}^{(t+2\pi/\omega)} e_\mathrm{m} (E_\mathrm{p} \sin \omega t + \eta_\mathrm{p} \omega \cos \omega t) \, e_\mathrm{m} \omega \cos \omega t \cdot \mathrm{d}t$$

$$= e_\mathrm{m}^2 \left[\frac{E_\mathrm{p}}{2} \sin^2 \omega t + \eta_\mathrm{p} \omega (\tfrac{1}{2} \omega t + \tfrac{1}{4} \sin 2 \omega t) \right]_{t}^{(t + 2\pi/\omega)}$$

$$= \tfrac{1}{2} e_\mathrm{m}^2 \cdot 2\pi \eta_\mathrm{p} \omega \tag{16.24}$$

The expression may be rearranged to give alternative forms

(energy loss/radian) per unit volume

$$= {}^1\!/_2 \; e_\mathrm{m}^2 \, \eta_\mathrm{p} \omega = {}^1\!/_2 \, f_\mathrm{m}^2 \, \frac{\eta_\mathrm{p} \omega}{(E_\mathrm{P}^2 + \eta_\mathrm{P}^2 \omega^2)} = {}^1\!/_2 f_\mathrm{m} e_\mathrm{m} \sin \delta \tag{16.25}$$

This indicates why δ is referred to as a loss angle. The representation in this form is important because it shows that, when the out-of-phase component is large (high values of tan δ or $\eta_\mathrm{p}\omega$), then there will be considerable energy dissipation, with consequent heating, if the material is subject to cyclic loading.

Representation (6)

For further mathematical development of the subject, the use of complex number notation is useful, just as it is in alternating current electricity.

With $i = \sqrt{(-1)}$, we can put:

$$\boldsymbol{e} = e_\mathrm{m} \exp(i\omega t) = e_\mathrm{m}(\cos \omega t + i \sin \omega t) \tag{16.26}$$

Our earlier basic relation, $e = e_\mathrm{m} \sin \omega t$, thus corresponds to the imaginary part of the above expression. If we follow through the analysis, and, at the end, take the imaginary part, this will therefore represent the behaviour of the system[1].

We now introduce a complex modulus $\boldsymbol{E}$ with a real part E' and an imaginary part E'': $\boldsymbol{E} = E' + i\,E''$. By the usual definition of a modulus, we have:

$$\boldsymbol{f} = \boldsymbol{E}\boldsymbol{e} = (E' + iE'') \, e_\mathrm{m} \exp(i\omega t)$$

$$= e_\mathrm{m}(E' \cos \omega t - E'' \sin \omega t) + i e_\mathrm{m}(E' \sin \omega t + \mathrm{E}'' \cos \omega t) \tag{16.27}$$

The imaginary part of this expression, $e_\mathrm{m}(E' \sin \omega t + E'' \cos \omega t)$, is identical in form to the expression for f in equations (16.11) and (16.15), so that the equivalence of the representation is proved. The parameters of this representation, which is very widely used, are:

[1]For this representation, though not for the others, it would have been simpler to shift the time origin, which is immaterial in the steady-state situation, and to use $e = e_\mathrm{m} \cos \omega t$. The real part of the complex quantities would then correspond to the actual ('real') behaviour. But, since the $\exp(i\omega t)$ factor is dropped anyway in analysis, there is no great harm in the other notation.

real part of modulus (often termed real modulus)

$$= E' = E_p = E \text{ as defined above} \tag{16.28}$$

imaginary part of modulus (often termed imaginary modulus or loss modulus)

$$= E'' = \eta_p\omega = E' \tan \delta \tag{16.29}$$

The advantage of this approach for mathematical purposes is that the factor exp ($i\omega t$) can be omitted and the analysis performed with the modulus in either the vector or the complex form:

$$\boldsymbol{F} = \boldsymbol{Ee} = (E' + i\,E'')\mathbf{e} \tag{16.30}$$

At the end of the analysis, the real part gives the in-phase component and the imaginary part the out-of-phase component. This is particularly valuable in dealing with composite systems or complex geometries. The same rules apply as in Hookean elasticity.

Summary of representations

The interrelations of the various representations are conveniently summarised by the vector diagram (Fig. 16.45). We note the identity of E, E_p and E', which are often referred to as the *storage modulis* because they define energy stored and recovered, and the identity of E'' and $\eta_p\omega$, referred to as the *loss modulis* representing dissipated energy, and their close relation to tan δ. One extreme situation occurs when there is ideal elasticity, $\eta_p\omega = 0$; the stress is in phase with strain, and there is no energy loss. The other extreme occurs with pure viscosity, with $E_p = 0$, the stress 90° out of phase, and a large energy loss. The relations, together with the intermediate situation, are illustrated in Fig. 16.46.

The use of more complicated spring and dashpot models in an attempt to represent the complete behaviour of fibres, as distinct from a response at a single frequency, is discussed in Section 20.7.1.

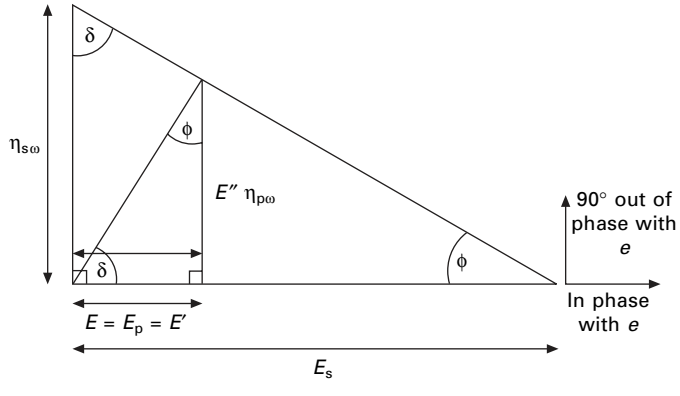

16.45 Summary of representations of linear viscoelasticity.

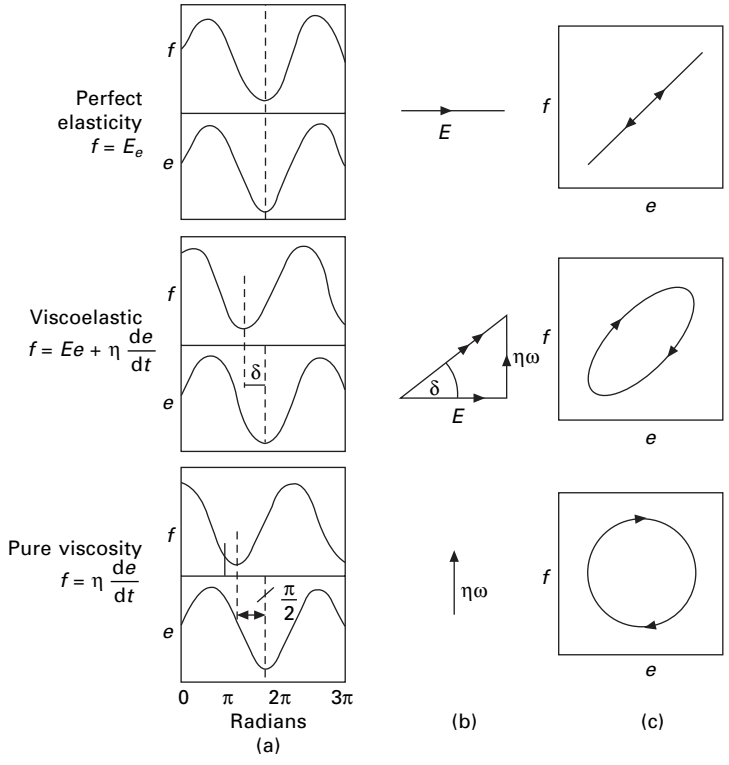

16.46 Representation of perfectly elastic, purely viscous and viscoelastic materials: (a) relations between sinusoidal stress and strain; (b) vector diagram; (c) stress–strain curve.

Table 16.6 Frequency range of dynamic tests

Method	Frequency range
Direct observation of stress–strain loop	up to 10 Hz
Free vibrations	1–50 Hz
Forced resonant vibration	1–300 Hz
Direct observation of forced vibrations	1–200 Hz
Flexural resonance of specimen (see Section 17.2.3)	20 Hz–10 kHz
Velocity of sound waves – continuous	500 Hz–30 kHz
Pulse velocity	10–100 kHz

16.5.3 Methods of dynamic testing

A variety of methods may be used in dynamic testing. The frequencies for which the methods described below have been used are given in Table 16.6.

Direct observation of stress–strain loop

At low frequencies (up to about 10 Hz), the methods described in Section 13.4 may be adapted to impose cyclic loading or extension and to record the stress–strain loop

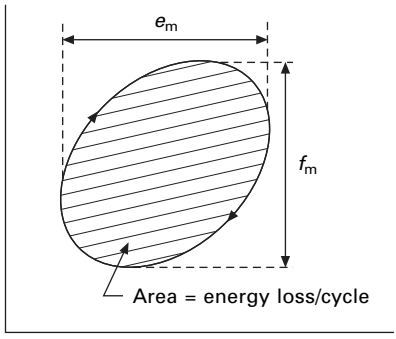

16.47 Hysteresis loop obtained in stress–strain test.

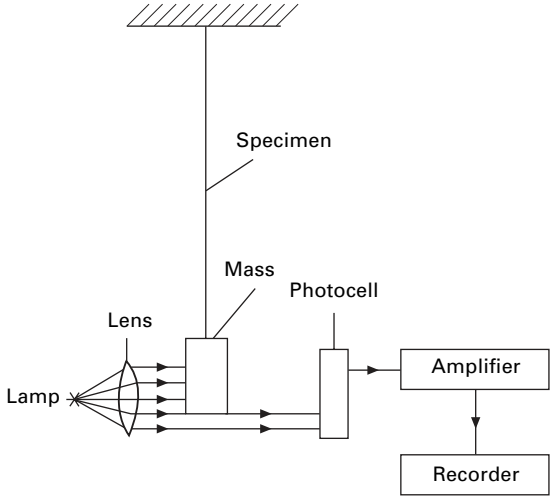

16.48 Oscillations of a free mass attached to a fibre.

directly. The values of f_m, e_m and the energy loss are simply found from the loop as shown in Fig. 16.47, and hence the other parameters can be calculated. As has been stated, this is really a quasi-static method.

Free vibrations

A truly dynamic method available over much the same frequency range is the study of the free vibrations of a mass suspended by a filament. Figure 16.48 illustrates the method used by Ballou and Smith [53]. The vibrations of the mass modulate the amount of light received by the photocell, and thus the frequency and damping of the oscillation may be followed on the recorder. A linear variable differential transformer (LVDT) or laser measurement of displacement could now be used in this method.

If A is the area of cross-section, l the length of the specimen and x its extension beyond its rest position, the restoring force will be given by substituting $x = el$ in equation (16.14) and multiplying the stress f by A. The equation of motion of the system is therefore:

$$m\frac{\mathrm{d}^2x}{\mathrm{d}t^2} - \eta_\mathrm{p}A\frac{1}{l}\frac{\mathrm{d}x}{\mathrm{d}t} - E_\mathrm{p}A\frac{x}{l} = 0 \tag{16.31}$$

where m is the suspended mass.

This is a damped simple harmonic motion, which will have a frequency given by:

$$\omega = \left(\frac{E_\mathrm{p}A}{ml} - \frac{\eta_\mathrm{p}^2A^2}{4m^2l^2}\right)^{1/2} \tag{16.32}$$

and a logarithmic decrement[2] given by

$$\lambda = \frac{\pi\eta_\mathrm{p}A}{\omega ml} \tag{16.33}$$

From these expressions, E_p and η_p can be calculated. If the damping is small, the following approximate relations hold:

$$E_\mathrm{p} = \frac{ml}{A}\omega^2 \tag{16.34}$$

$$\eta_\mathrm{p} = \frac{\omega ml\lambda}{A} \tag{16.35}$$

In a similar method, Lincoln [54] recorded photographically the oscillations of an out-of-balance beam, one arm of which was connected to the specimen.

Van der Meer [55, 56] has used the free vibration of a torsion pendulum restrained by a pair of yarns, as illustrated in Fig. 16.49, to measure dynamic properties in air and water. At any instant, two yarn sections are extending and two are contracting, so that they are subject to a dynamic tensile loading.

Forced resonant vibrations

Alternatively, the specimen may be subjected to forced oscillations by means of an electromagnetic drive, as illustrated in Fig. 16.50. The equation of motion will then be:

$$m\frac{\mathrm{d}^2x}{\mathrm{d}t^2} - \eta_\mathrm{p}A\frac{1}{l}\frac{\mathrm{d}x}{\mathrm{d}t} - E_\mathrm{p}A\frac{x}{l} = F\cos\omega t \tag{16.36}$$

where F = amplitude of the applied force and ω = frequency of the forced vibration.

If the amplitude of the vibration is plotted against the frequency, it will give a resonance curve. The resonant frequency is given by:

$$\omega_0^2 = \frac{E_\mathrm{p}A}{ml} \tag{16.37}$$

and the width of the resonance curve, when the amplitude of the vibration is $1/\sqrt{2}$ times its maximum value, by:

[2]If x_1 and x_2 are successive maxima of the vibration in the same direction, the logarithmic decrement is defined by the relation $x_1/x_2 = \mathrm{e}^\lambda$.

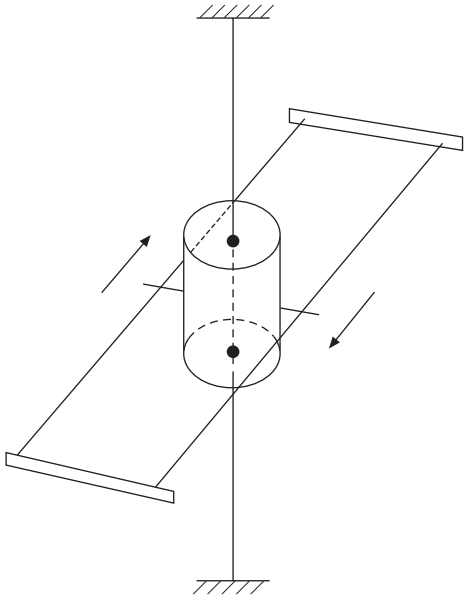

16.49 Torsion pendulum as used for tensile dynamic oscillation by van der Meer [55, 56].

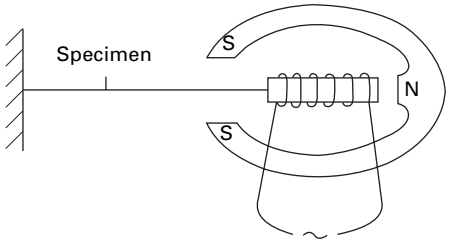

16.50 Forced oscillations with electromagnetic drive.

$$\Delta\omega = \frac{\eta_p A}{2ml} \tag{16.38}$$

Thus the parameters E_p and η_p can be calculated. If the damping is large, slightly more complicated expressions must be used to find E_p and η_p.

A method suitable for use with single filaments between 1 and 100 Hz has been described in detail by Dunell and Dillon [57], and a similar method has been used by Tipton [58].

The vibrator consists of a solenoid of fine wire wound on a paper core and mounted in a magnetic field. Dunell and Dillon also discussed the corrections needed to take account of the frictional resistance and elastic reaction of parts of the vibrator itself. The use of this method is limited to conditions in which the length of the specimen is much less than the wavelength of the propagated wave. At high frequencies, the specimen must be short.

Direct observation of forced vibrations

Probably the most widely used method is the direct observation of forced vibrations by means of the apparatus developed by Takayanagi [59, 60] (marketed as the *Rheovibron* tester) or similar procedures with newer transducers and digital recording and analsyis. These instruments are often referred to as dynamic mechanical analysers (DMA). The *Universal Fibre Tester* [61, 62], which was derived from a fatigue tester described in Section 19.3, is an instrument that can be used in the same way.

The principle of the method is illustrated in Fig. 16.51. An oscillator, which can be set at various frequencies, typically 110 Hz, excites a vibrator, which subjects the fibre to a cyclic strain. A transducer at the other end of the fibre detects the resulting tension variation. The outputs from the load transducer and a strain transducer are fed to appropriate electronic circuits; and the values of the ratio of load to elongation and of tan δ are directly indicated or recorded. Means of varying temperature are incorporated in the *Rheovibron* tester.

Velocity of sound: continuous transmission

At higher frequencies, the inertia of the specimen itself cannot be neglected, and the methods used must take account of this. The problem is essentially one of measuring the velocity of longitudinal (sound) waves in the specimen. The method was first applied by Lotmar [63], who excited the specimen by friction and matched the note produced with that of a standard specimen. Later, Ballou and Silverman [64] investigated the standing waves set up for certain positions of a reflecting pickup when one end of a filament was excited with a known frequency.

Probably the best method is the interference method adopted by Ballou and Smith [53], which could now be modified by analogue to digital conversion and signal processing. As illustrated in Fig. 16.52, one end of the specimen is excited electromagnetically, and consequently sound waves travel along the specimen and can be picked up by a piezo-electric crystal detector. The signal from the detector is amplified and filtered and fed into a cathode-ray oscilloscope (CRO), together with

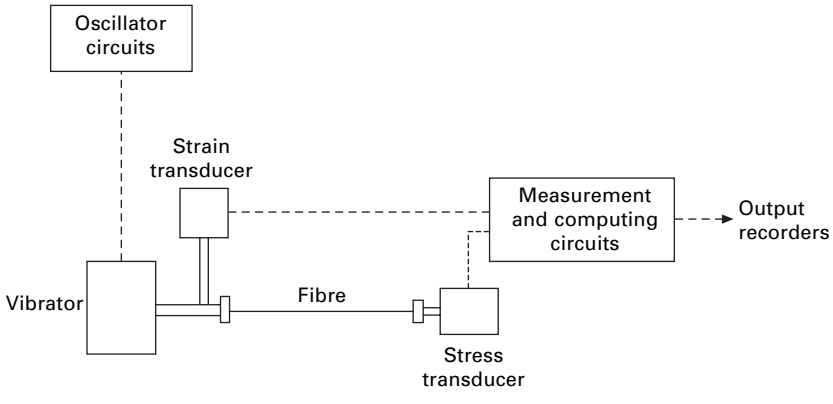

16.51 Principle of *Rheovibron* tester.

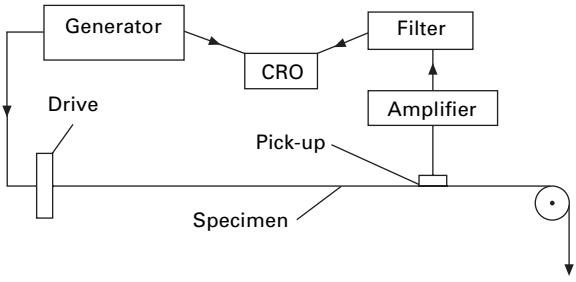

16.52 Interference method for finding velocity of sound waves.

a signal direct from the generator. The resultant trace on the oscilloscope will depend on the difference in phase of the two signals and will be a maximum whenever the two are in phase. Thus, as the pick-up is moved along the specimen, an interference pattern of maxima and minima will be observed. The time taken for the waves to travel the distance between successive maxima must be equal to the period of the oscillation. Therefore:

$$c = L\left(\frac{\omega}{2\pi}\right) \tag{16.39}$$

where c = velocity of sound waves in cm/s, L = distance moved by pick-up between successive maxima and $(\omega/2\pi)$ = frequency in Hz.

If the damping is small, the velocity of sound in a medium is given by:

$$c^2 = \frac{E}{\rho} \tag{16.40}$$

where ρ = density. Thus the value of the dynamic modulus may be calculated. The specific modulus is equal to c^2.

From the attenuation of sound along the specimen, which will be given by the reduction in amplitude of the interference pattern on the oscilloscope, we get:

$$\eta = \frac{2\rho\alpha c^3}{\omega^2} \tag{16.41}$$

where α = attenuation in nepers/cm.[3]

If the damping is appreciable, these expressions must be modified. Corrections must also be included for the effect of standing waves owing to reflection from the end of the specimen. The full expressions are given in the paper by Ballou and Smith [53].

A similar method was used by Hillier and Kolsky [65, 66], but they compared the transmitter and receiver signals connected to separate beams of a double-beam oscilloscope.

[3]Neper (Np) = $\log_e (x_1/x_2)$, where x_1 and x_2 are successive values of amplitude (in this case at 1 cm intervals). The neper is analogous to the decibel, which is based on log10. 1 Np = 8.686 decibel.

Pulse-velocity methods

Instead of exciting the whole specimen into continuous vibration, one may measure the velocity of a train of waves of known frequency by determining the time taken for a short pulse to travel along the specimen. This method has been used by Chaikin and Chamberlain [67] at 100 kHz. The circuit arrangements indicated in Fig. 16.53 illustrate the basic principles, but later instruments use other transducers, electronics and information technology.

A brief pulse of the required frequency is transmitted along the specimen from a crystal of Rochelle salt and eventually arrives at the receiver, which is a condenser microphone. The time of travel is measured by a method similar to that used in recording echo pulses in radar systems. At the instant that the pulse is transmitted, the two beams of a cathode-ray oscilloscope are released and start to travel at constant speed across the screen. The receiver is connected to one of the beams and a mark appears on the trace at the instant at which the pulse arrives. A timing unit is connected to the other beam to give a series of time marks. Thus the time taken for the pulse to travel can be found from a photograph of the traces.

In order to avoid errors due to delays in the circuit, the time taken for travel along specimens of varying length is determined. The slope of the graph of time against length, determined by the method of least squares, then gives the velocity of travel of the pulse. Young's modulus is given by equation (16.40): $E = \rho c^2$. The method is not suited to the measurement of attenuation, so the viscous parameter η cannot be found.

Another apparatus, incorporating two transducers, transmitter and receiver, that touch the specimen and an electronic circuit to measure the time interval for the pulse to travel from one to the other, has been described by Hamburger [68] and used by Moseley [69, 70]. It is commercially available as a pulse propagation meter (PPM). Some care is needed in the interpretation of results of pulse propagation tests, since at 10 kHz, as used by Moseley, and a typical recorded sonic velocity of 1 km/s, the wavelength will be 10 cm. This is about the distance apart of the transducers, so that

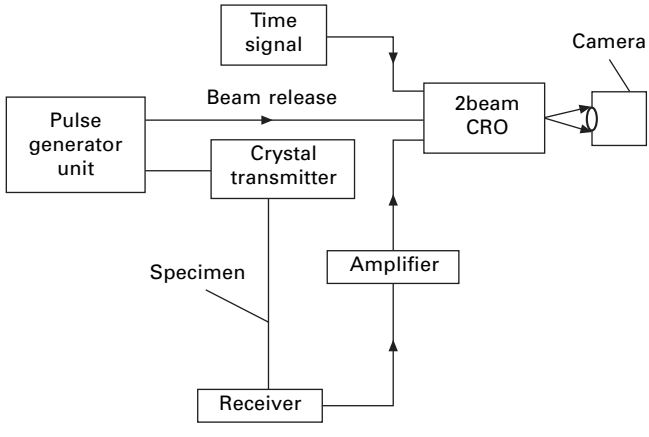

16.53 Pulse-velocity method.

the measurement is one not of a short pulse of waves travelling along the specimen, but of the times between the triggering of the transducers by the transient at the beginning of the pulse. This is a complex situation, which makes the true test frequency unknown and can lead to error if the pulse changes in shape during transmission. At higher frequencies, as used by Chaikin and Chamberlain [67], the error will be less. Mi [41] modified the PPM to have receivers at different distances on either side of the transmitter, which eliminated any errors associated with time detection differences at transmitter and receiver and allowed attenuation to be determined.

16.5.4 Cyclic dynamic modulus

The fact that the dynamic storage and loss moduli are not the constant values of the simple model is shown in studies by Bosman [71]. Figure 16.54(a) shows cyclic loading plots at different positions on the load–elongation curve of a high-tenacity polyester yarn. The continuing shift of the hysteresis loops is due to creep. Other tests were carried out a constant strain amplitudes. Figure 16.54(b) shows that the moduli change with number of cycles, the storage modulus increasing and the loss factor (tan δ) decreasing. Figure 16.55(a) shows that the dynamic modulus E' increases with increasing mean load and decreases with increasing strain amplitude. Figure 16.55(b) shows that the loss modulus E'' is independent of mean load but increases with strain amplitude. The latter effect has important consequences for heating when large fibre assemblies, such as ropes, are cyclically loaded. Not only is there a direct effect of the increased amplitude but the rise in E'', which is also shown in a plot of tan δ, means that a larger fraction of the input energy is dissipated as heat. Tan δ increases from 0.006 at 0.25% strain amplitude to 0.15 at 2%, a 25-fold increase.

Selden and Dartman [26] report the values for nylon 6 given in Table 16.7. The most consistent effects are an increase in both E' and E'' with pre-load, a decrease in E' and an increase in E'' with dynamic strain. Values of tan δ are only slightly higher at the higher dynamic strain.

16.5.5 Values of dynamic modulus

The relation of the dynamic modulus (sonic modulus) to the moduli determined by a stress–strain test is illustrated by the results of Charch and Moseley [69], shown in Fig. 16.56. For an *Orlon* acrylic fibre yarn, the dynamic modulus, measured with a 10 kHz pulse, had a value of 14.7 N/tex, which was somewhat larger than the value of 12.4 N/tex observed for the initial modulus in a stress–strain test at 1700% per second, and considerably larger than the value of 7.9 N/tex found at 1/60% per second (1% per minute). Similar results were obtained for other fibres.

In continuing extension, the incremental modulus given by the slope of the curve decreases markedly at the yield point. By contrast, the dynamic modulus, which shows up the response to a superimposed oscillation, usually increases. Even up to strains as small as 1%, Chaikin and Chamberlain [67] found a small but significant increase in the dynamic modulus of nylon, though the values for wool and hair were constant.

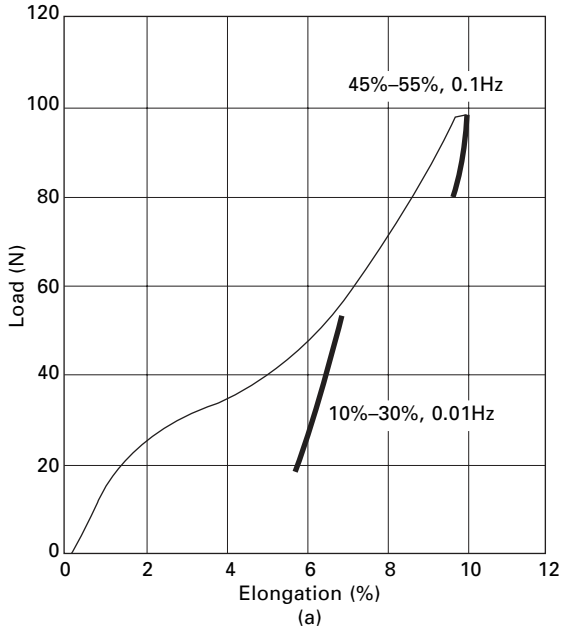

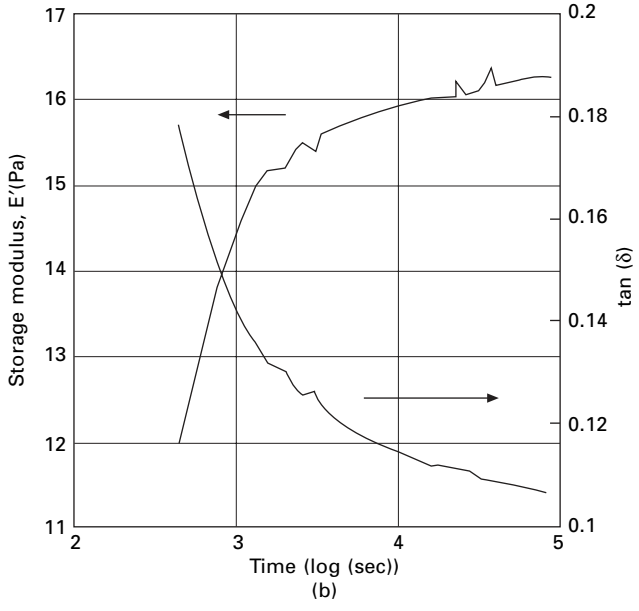

16.54 (a) Cyclic loading at percentage of break load and frequency indicated at different parts of the stress–strain curve of high-tenacity polyester yarn showing also some creep in successive cycles. (b) Change in dynamic modulus E and tan δ with time at 0.1 Hz, 30% of mean break load and 2% strain amplitude. From Bosman [71].

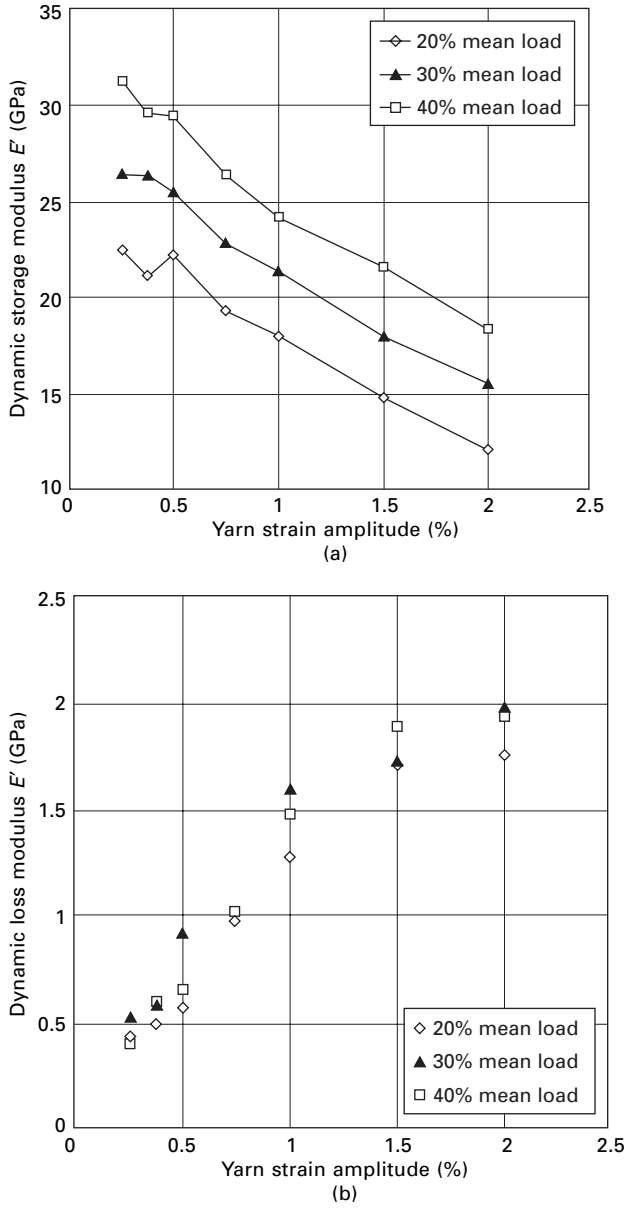

16.55 Change in (a) dynamic modulus E' and (b) loss modulus E'' of high-tenacity polyester yarn after 10 000 cycles at various mean loads and strain amplitudes.

Figure 16.57 shows results obtained by de Vries [72] for a variety of regenerated-cellulose fibres. The variation of dynamic modulus with extension falls into two parts: up to a critical strain, e_c, the modulus is constant, with a value E, but above this value it increases linearly with strain. The critical values for the various fibres fall on a curve given by:

Table 16.7 Dynamic moduli of nylon 6 fibres. Based on Selden and Dartman [26]

Pre-load (mN/tex)	*E′* (GPa)			*E″* (GPa)			tanδ		
	0.1 Hz	1 Hz	10 Hz	0.1 Hz	1 Hz	10 Hz	0.1 Hz	1 Hz	10 Hz
Dynamic strain = ± 1%									
27	1.39	1.69	1.97	0.32	0.37	0.34	0.23	0.22	0.17
45	2.56	2.71	3.14	0.54	0.64	0.58	0.21	0.24	0.18
91	2.58	3.55	4.14	0.82	0.77	0.59	0.32	0.22	0.14
182	5.14	7.28	8.19	1.15	0.96	0.75	0.22	0.12	0.09
Dynamic strain = ± 2%									
27	1.08	1.56	1.78	0.27	0.40	0.40	0.25	0.26	0.22
45	1.45	2.00	2.25	0.37	0.51	0.49	0.26	0.26	0.22
91	1.77	2.63	3.08	0.58	0.54	0.51	0.33	0.19	0.11

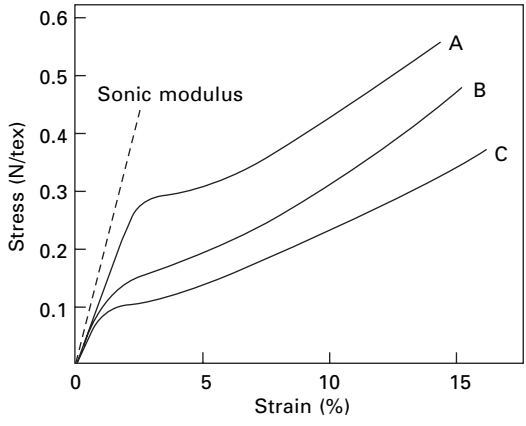

16.56 Stress–strain curves of *Orlon* acrylic fibre yarn at rates of strain of: A, 1700; B, 1.7; C, 0.017% per second, showing relation of initial slope to dynamic modulus [69].

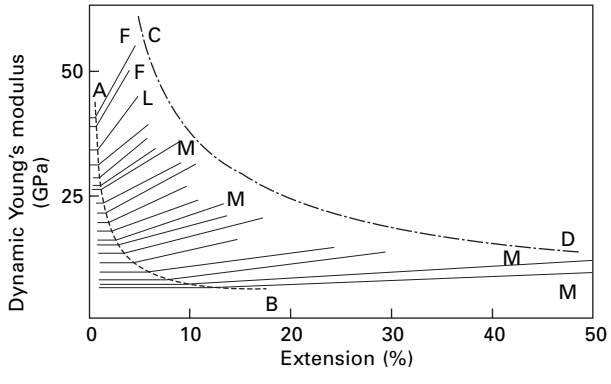

16.57 Dynamic modulus of cellulose fibres. AB is locus of e_c. CD is locus of breaking extensions in tensile tests. F, saponified acetate; L, Lilienfield rayon; M, model filament; remainder are viscose rayon [72].

$$E_c \cdot e_c^{0.63} = 1.73\,\text{kN/mm}^2 \tag{16.42}$$

The critical strain e_c is found to be more nearly equal to the yield point given by recovery experiments than to that given by the shape of the stress–strain curve. De Vries also found that, during relaxation of stress at constant extension, the dynamic modulus changed very little, and not at all after the first 30 s, even though the stress decreased by as much as 30%. Measurements of dynamic modulus during load–extension tests carried out at various rates also indicate that the dynamic modulus reaches equilibrium in less than a minute as a single-valued function of the strain. This value is independent both of the particular stress-history of the specimen leading to the given strain and of the value of the stress in the specimen at the time of measurement. It was, however, found that only values of E above the critical strain were reversible; once a specimen had been extended into the range of increasing E, the initial constant portion of the curve was not repeated.

Figure 16.58 shows values obtained by Tipton [58] for a variety of textile yarns. He also found that the dynamic modulus fell slightly and that the loss factor increased as the amplitude of the dynamic strain was increased.

The orientation and crystallinity of the specimen will have a considerable influence on the dynamic modulus. Table 16.8 shows the various types of regenerated-cellulose filaments studied by de Vries, together with the values of the dynamic modulus at low strain. The modulus is much greater in the more highly oriented specimens. The effects of both crystallinity and orientation in *Dacron* polyester are shown in Table 16.9, which presents data obtained by Ballou and Smith [53]. Other values, obtained by the pulse propagation technique, have been reported by Dumbleton [73].

If other factors are unchanged, the dynamic modulus can be used as a measure of orientation; but care must be taken, since many treatments, for example, the effect of annealing or hot stretching of synthetic fibres, change the structure in other ways, which also influence the modulus. It must be remembered that all one is measuring

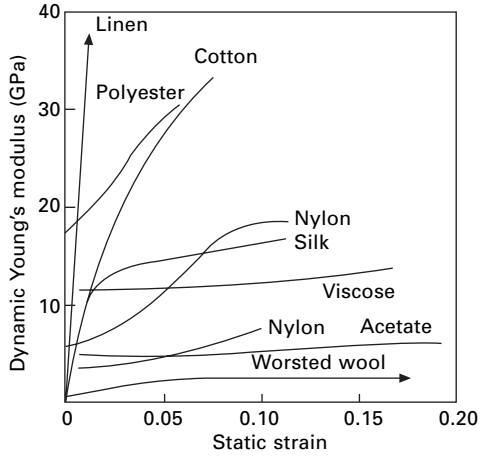

16.58 Dynamic modulus with static strain for various textile yarns [58].

Table 16.8 Dynamic modulus of regenerated-cellulose filaments at 8.8 kHz [72]

Material	*E*c (GPa)
Nearly isotropic model filaments	5.4
Stretched model filaments	5.4–23
Viscose rayons of low, medium and high tenacity	8–20
Very high-tenacity viscose rayon	20–30
Lilienfeld rayon	35
Fortisan	40

Table 16.9 Viscoelastic constants of poly(ethylene terephthalate) [53]

Frequency	Orientation	Crystallinity	*E* (GPa)	η (N s/mm^2)	$\tau = \eta/E$ (μs)
8 Hz	None	None	2.3	1.11	480
8 Hz	None	High	0.95	0.53	560
8 Hz	High	None	11.4	4.67	410
8 Hz	High	Low	12.0	6.48	540
8 kHz	High	Low	15.3	0.020	1.3
12 kHz	High	Low	15.3	0.012	0.8
16 kHz	High	Low	15.3	0.008	0.55
34 kHz	High	Low	16.3	0.007	0.45

in determining the dynamic modulus is the response of the fibre as a whole to a rapid cyclic extension.

16.5.6 Transitions in dynamic moduli

There are many mechanisms by which a fibre can deform. Some of these, such as the stretching of atomic bonds, are characterised by large stresses and small strains but occur at very high speed; others, such as the uncoiling of chains, lead to large strains under low stresses but take a long time owing to viscous drag. The typical effect of one of these mechanisms on the dynamic moduli is illustrated by the simple model shown in Fig. 16.59(a). At high frequencies, only the stiff mechanism operates and the modulus is high, but at low frequencies the soft mechanism can operate and the modulus is low. At the extremes, there is little energy loss: at high frequencies, there is little viscous displacement; at low frequencies, there is little viscous resistance. But near the transition, when the structure is just becoming mobile, the viscous resistance is very important in causing a large energy loss, or, what comes to the same, in causing a large phase lag. The 'loss' quantities (E'', $\eta_p\omega$, $\tan\delta$) will therefore go through a maximum, as shown in Fig. 16.59(b). With a variety of mechanisms, a sequence of drops in E' and peaks in E'' can be expected. Unfortunately, there are no studies of fibres over a wide enough range of frequencies to enable one to plot experimental data analogous to Fig. 16.59(b). However, it is found that the modulus increases with frequency; for example, Chaikin and Chamberlain [67] obtained the comparative values given in Table 16.10. This table also includes some data from other sources.

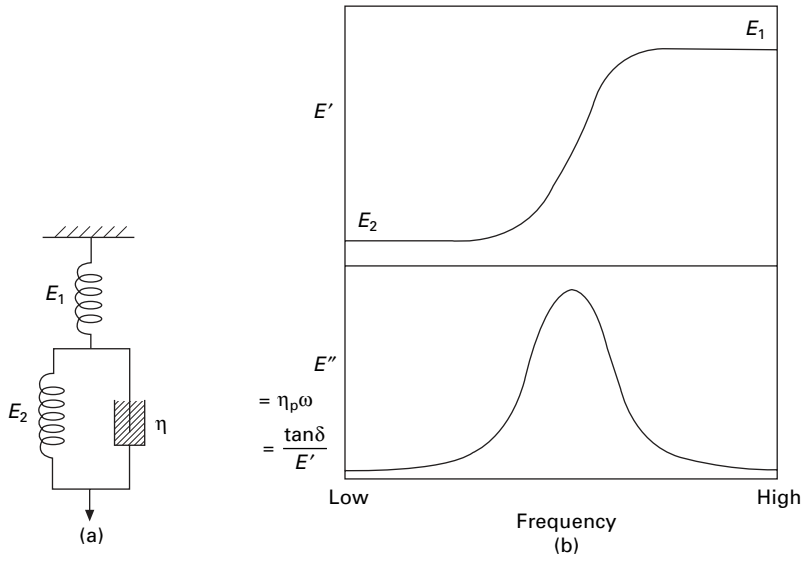

16.59 (a) Simple model of viscoelastic behaviour. (b) Real and imaginary moduli of model.

Table 16.10 Dynamic modulus values

Fibre	E' (GPa)				E'' (GPa)
	Static [67]	1.5–100 Hz [57]	10 kHz [68]	100 kHz [67]	1.5–100 Hz [57]
Viscose rayon	4.2	10.6	17.1	19.5	0.48
Wool	3.1			8.6	
Nylon	2.9	5.8	8.5	7.0	0.38
Steel	1.93			1.98	

It is possible, however, to observe the transitions by causing the structure to loosen up, to become mobile, for oscillations of a given frequency. This can be achieved by raising the temperature, so that thermal vibrations become more effective, or by plasticising the structure, most easily with water, so that the intermolecular forces are reduced.

The thermal transitions will be discussed in detail in Chapter 18, but one example is given here. Figure 16.60 shows the changes in the real and imaginary (loss) modulus of nylon 6.6 fibres with a transition at about 90 °C.

The transitions in dynamic properties can also be studied in bending or torsion, as will be described in the next chapter.

16.5.7 Strain-wave propagation: limiting impact velocity

At very high rates of extension, or impact, the tension wave (or stress wave) and the associated strain wave take a significant time to travel along the fibre. Smith *et al.*

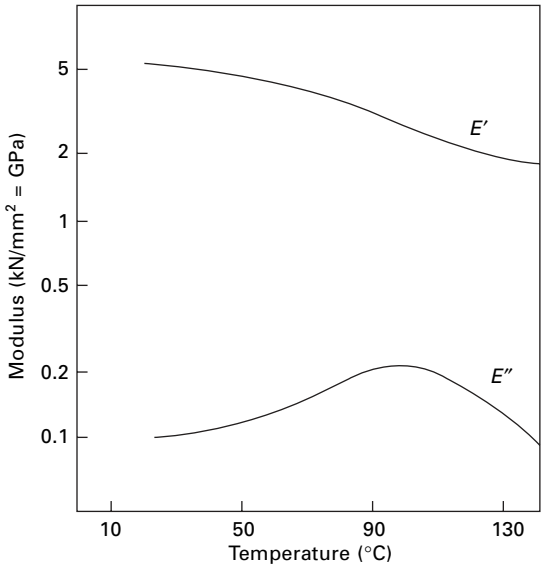

16.60 Real and imaginary dynamic moduli of nylon 6.6 fibres. From Murayama *et al.* [23].

[33] have studied the propagation of strain waves along yarns. The theory and the interpretation of data are complicated, but the order of magnitude of the effects can be indicated by noting that the strain wave front velocity is about 3900 m/s in a polyester fibre yarn and 2800 m/s in a nylon yarn. A comparison of experimental results with a theoretical prediction suggested that appreciable creep and stress relaxation occurred within 50 μs of impact but that there was no creep or stress relaxation between 50 and 300 μs. The very rapid effects will, of course, be due to different mechanisms from the slow creep and relaxation discussed previously. Mi [41], using the PPM found similar values for the wave velocity in polyester and nylon and 7500 m/s in aramid (*Kevlar*). Attenuation of the signal was as $\exp(-\eta L)$, where η is the attenuation coefficient and L is the length travelled, so that there is a decrease of 0.37 times in a length $1/\eta$. The values of $1/\eta$ were: nylon, 2.3 m; polyester, 3.4 m; aramid 20 m.

As the speed of impact is increased, a point is reached at which the material is unable to accommodate the rapid displacement of the end of the specimen by propagating strain along the specimen. There is thus a critical velocity at which the specimen breaks on impact. Smith *et al.* [74] have shown how the critical velocity may be estimated from stress–strain curves. The estimated values lie between 100 and 300 m/s for different yarns and are generally greater in fibres with an appreciable region of low modulus at the high level of extension before break.

16.6 References

1. N. J. Abbott. *Text. Res. J.*, 1951, **21**, 227.
2. M. T. O'Shaughnessy. *Text. Res. J.*, 1948, **18**, 263.

3. J. J. Press. *J. Appl. Phys.*, 1943, **14**, 224.
4. H. Leaderman. *Elastic and Creep Properties of Filamentous Materials and Other High Polymers*, the Textile Foundation, Washington, DC, 1943.
5. E. Catsiff, T. Alfrey and M. T. O'Shaughnessy. *Text. Res. J.*, 1953, **23**, 808.
6. R. L. Steinberger. *Text. Res.*, 1936, **6**, 191, 267.
7. M. Feughelman. *J. Text. Inst.*, 1954, **45**, T630.
8. O. Ripa and J. B. Speakman. *Text. Res. J.*, 1951, **21**, 215.
9. R. Meredith and F. T. Peirce. *J. Text. Inst.*, 1948, **39**, T159.
10. W. J. Lou and C. I. Tseng., *Polymer Composites*, 1997, **18**, 492.
11. TTI and Noble Denton. *Deepwater Moorings: An Engineer's Guide*, Oilfield Publications, Ledbury, 1999.
12. L.E. Govaert. PhD thesis, Eindhoven University of Technology, 1990.
13. M. J. N. Jacobs. PhD thesis, Eindhoven University of Technology, 1999.
14. D. J. Dijkstra and A. J. Pennings. *Polymer Bulletin*, 1988, **19**, 75.
15. M. A. Wilding and I. M. Ward., Polymer, 1978, **19**, 919.
16. I. M. Ward. Polymer Eng. Sci., 1984, **24**, 724.
17. L. E. Govaert, C. W. M. Bastaansen and P. J. R. Libland. *Polymer*, 1993, **34**, 534.
18. R. Meredith. *J. Text. Inst.*, 1954, **45**, T438.
19. S. M. Katz and A. V. Tobolsky. *Text. Res. J.*, 1950, **20**, 87.
20. M. Feughelman. *Appl. Polymer Symp.*, 1971, No. **18**, 757.
21. G. C. Wood. *J. Text. Inst.*, 1954, **45**, T462.
22. R. Meredith and B. Hsu. *J. Polymer Sci.*, 1962, **61**, 253.
23. T. Murayama, J. H. Dumbleton and M. L. Williams. *J. Macromol. Sci. (Phys.) B*, 1967, **1**, 1.
24. T. Murayama, J. H. Dumbleton and M. L. Williams. *J. Polymer Sci. A–2*, 1968, **6**, 787.
25. P. R. Pinnock and I. M. Ward. *Polymer*, 1966, **7**, 255.
26. R. Selden and T. Dartman. *Textile Res. J.*, 1998, **68**, 264.
27. J. G. M. van Miltenburg. *Textile Res. J.*, 1991, **61**, 363.
28. R. P. Nachane and V. Sundaram. *J. Textile Inst.*, 1995, **86**, 10.
29. R. P. Nachane and V. Sundaram. *J. Textile Inst.*, 1995, **86**, 20.
30. R. Meredith. *J. Text. Inst.*, 1954, **45**, T30.
31. W. J. Lyons and I. B. Prettyman. *Text. Res. J.*, 1953, **23**, 917.
32. H. F. Schiefer, W. D. Appel, J. F. Krasny and G. G. Richey. *Text. Res. J.*, 1953, **23**, 489.
33. J. C. Smith, C. A. Fenstermaker and P. J. Shouse. *Text. Res. J.*, 1965, **35**, 743.
34. J. C. Smith, C. A. Fenstermaker and P. J. Shouse. *Text. Res. J.*, 1963, **33**, 919.
35. I. H. Hall, *J. Polymer Sci. A–2*, 1967, **5**, 1119.
36. G. Holden. *J. Text. Inst.*, 1959, **50**, T41.
37. J. C. Smith, F. L. McCrackin, H. F. Schiefer, W. K. Stone, and K. M. Towne. *Text. Res. J.*, 1956, **26**, 281.
38. W. K. Stone, H. F. Schiefer and G. Fox. *Text. Res. J.*, 1955, **25**, 520.
39. F. L. McCrackin, H. F. Schiefer, J. C. Smith, and W. K. Stone. *Text. Res. J.*, 1955, **25**, 529.
40. J. C. Smith, F. L. McCrackin, and H. F. Schiefer. *Text. Res. J.*, 1955, **25**, 701.
41. Z. X. Mi. PhD thesis, University of Manchester, 1983.
42. G. W. H. Stevens and F. C. Bluett. Aeronautical Research Council, Current Papers, No. 1061, 1969.
43. G. W. H. Stevens and J. C. H. Longrigg. RAE Technical Report, No. 69108, 1969.
44. I. Marshall and A. B. Thompson. *Proc. Roy. Soc.*, 1954, **A221**, 541.
45. T. A. Godfrey. *J. Textile Inst.*, 2001, **92**, 16.
46. R. Meredith. In *Fibre Science*, J. M. Preston (Editor), The Textile Institute, Manchester, 2nd edition, 1953, p. 260.
47. J. L. J. van Dingenen. In *High-performance Fibres*, J. W. S. Hearle (Editor), Woodhead Publishing, Cambridge, 2001, p. 62.

48. P. Schwartz, A. Netravali and S. Sembach. *Textile Res. J*., 1986, **56**, 502.
49. J. Sikorski and H. J. Woods. *Proc. Leeds Phil. Soc.*, 1950, **5**, 313.
50. I. H. Hall. *J. Appl. Polymer Sci.*, 1968, **12**, 731, 739.
51. J. C. Smith, P. J. Shouse, J. M. Blandford and K. M. Towne. *Text. Res. J.*, 1961, **31**, 721.
52. J. Skelton, W. D. Freeston and H. K. Ford. *Appl. Polymer Symp.*, 1969, No. **12**, 111.
53. J. W. Ballou and J. C. Smith. *J. Appl. Phys.*, 1949, **20**, 493.
54. B. Lincoln. *J. Text. Inst.*, 1952, **43**, T158.
55. S. J. van der Meer. Doctoral Thesis, Delft, Netherlands, 1970.
56. S. J. van der Meer. *J. Text. Inst.*, 1974, **65**, 288.
57. B. A. Dunell and J. H. Dillon. *Text. Res. J.*, 1951, **21**, 393.
58. H. Tipton. *J. Text. Inst.*, 1955, **46**, T322.
59. M. Takayanagi. *Mem. Fac. Engng Kyushu Univ.*, 1963, **23**, No. 1.
60. M. Takayanagi. In *Proceedings of Fourth International Congress of Rheology* E. H. Lee and A. L. Copley (Editors), Interscience, New York, 1965, Part I, p. 161.
61. A. R. Oudet, A. R. Bunsell, R. Hagege and M. Sotton. *J. Appl. Polymer Sci.*, 1984, **29**, 4363.
62. C. Le Clerc, A. R. Bunsell and A. Plant, *J. Materials Sci*., 2006, **41,** 750.
63. W. Lotmar. *Helv. Chim. Acta*, 1936, **19**, 68.
64. J. W. Ballou and S. Silverman, *Text. Res.*, 1944, **14**, 289.
65. K. W. Hillier and H. Kolsky. Proc. Phys. Soc., 1949, **B62**, 111.
66. K. W. Hillier. *Proc. Phys. Soc.*, 1949, **B62**, 701.
67. M. Chaikin and N. H. Chamberlain. *J. Text. Inst.*, 1955, **46**, T25, T44.
68. W. J. Hamburger. *Text. Res. J.*, 1948, **18**, 705.
69. W. H. Charch and W. W. Moseley, jr. *Text. Res. J.*, 1959, **29**, 525.
70. W. W. Moseley, jr. *J. Appl. Polymer Sci.*, 1960, **3**, 266.
71. R. L. Bosman. OCEANS 96 conference Institution of Electrical and Electronics Engineers and Marine Technology Society, Fort Laoderdale, Florida, OSA, 1996, September 23–26.
72. H. de Vries. *Appl. Sci. Res.*, 1952, **A3**, 111.
73. J. H. Dumbleton. *J. Polymer Sci. A–2*, 1968, **6**, 795.
74. J. C. Smith, J. M. Blandford, and K. M. Towne. *Text. Res. J.*, 1962, **32**, 67.